

UNIVERSITÉ DU QUÉBEC

**PRÉCISIONS SUR L'ANATOMIE DE L'OSTÉOLÉPIFORME  
*EUSTHENOPTERON FOORDI* DU DÉVONIEN SUPÉRIEUR  
DE MIGUASHA, QUÉBEC**

MÉMOIRE

PRÉSENTÉ À

L'UNIVERSITÉ DU QUÉBEC À RIMOUSKI

Comme exigence partielle du programme de Maîtrise en Gestion de la Faune  
et de ses Habitats

PAR

JOËL LEBLANC

Août 2005

UNIVERSITÉ DU QUÉBEC À RIMOUSKI  
Service de la bibliothèque

Avertissement

La diffusion de ce mémoire ou de cette thèse se fait dans le respect des droits de son auteur, qui a signé le formulaire « *Autorisation de reproduire et de diffuser un rapport, un mémoire ou une thèse* ». En signant ce formulaire, l'auteur concède à l'Université du Québec à Rimouski une licence non exclusive d'utilisation et de publication de la totalité ou d'une partie importante de son travail de recherche pour des fins pédagogiques et non commerciales. Plus précisément, l'auteur autorise l'Université du Québec à Rimouski à reproduire, diffuser, prêter, distribuer ou vendre des copies de son travail de recherche à des fins non commerciales sur quelque support que ce soit, y compris l'Internet. Cette licence et cette autorisation n'entraînent pas une renonciation de la part de l'auteur à ses droits moraux ni à ses droits de propriété intellectuelle. Sauf entente contraire, l'auteur conserve la liberté de diffuser et de commercialiser ou non ce travail dont il possède un exemplaire.

## TABLE DES MATIÈRES

TABLE DES MATIÈRES.....	ii
LISTE DES TABLEAUX.....	v
LISTE DES FIGURES.....	vi
INTRODUCTION GÉNÉRALE.....	xi
RÉFÉRENCES.....	xiv
REMERCIEMENTS.....	xvi

## CHAPITRE 1

### NEW DATA AND NEW METHODS ON AN OLD PROBLEM: THE CHOANA

<b>REVISITED.....</b>	<b>1</b>
ABSTRACT.....	2
RÉSUMÉ.....	3
INTRODUCTION.....	5
MATERIAL AND METHODS.....	8
RESULTS.....	9
<i>Phylogenetic analyses</i> .....	13
DISCUSSION.....	16
ACKNOWLEDGEMENTS.....	18
REFERENCES.....	19
Tables.....	23
Figures .....	25

## CHAPITRE 2

<b>DEVELOPMENTAL MODULARITY AND SALTATORY ONTOGENY IN THE LATE DEVONIAN OSTEOLEPIFORM <i>EUSTHENOPTERON FOORDI</i>.....</b>	<b>32</b>
ABSTRACT.....	33
RÉSUMÉ.....	34
INTRODUCTION.....	36
MATERIAL AND METHODS.....	39
<i>Specimens</i> .....	39
<i>Sequence of ossification</i> .....	39
<i>Measurements</i> .....	41
<i>Bone terminology</i> .....	41
RESULTS.....	42
<i>Skull</i> .....	43
<i>Sequences of ossification of the fins</i> .....	44
<i>Pectoral fins</i> .....	45
<i>Pelvic fins</i> .....	45
<i>First dorsal fin</i> .....	45
<i>Second dorsal fin</i> .....	46
<i>Anal fin</i> .....	46
<i>Vertebral column and caudal fin</i> .....	47
<i>Disparity and reliability of the sequence</i> .....	49
<i>Relative order of ossification of the fins</i> .....	52

<i>Basal scutes</i> .....	53
<i>Lepidotrichia</i> .....	54
<i>Ontogenetic pathway</i> .....	55
DISCUSSION.....	57
CONCLUSION.....	61
ACKNOWLEDGMENTS.....	62
REFERENCES.....	63
Tables.....	68
Figures .....	70
CONCLUSION GÉNÉRALE.....	85

## LISTE DES TABLEAUX

### Chapitre 1

**Table 1.** Relative dimensions of nasal capsule related structures among three specimens of *Eusthenopteron foordi*. All measurements are given in percentage; naris height: proportion of snout height (lateral view); naris depth: proportion of snout width (scan view); nasal capsule width: proportion of snout width; passage depth: proportion of snout height; choana width: proportion of snout width. .... 19

**Table 2.** Results of phylogenetic analyses using PAUP\*4.0b10 on four previously published matrices. .... 20

### Chapitre 2

**Table 1.** Major axis and 95% confidence interval for the slope for six fin position in relation to the standard length of *Eusthenopteron foordi* ( $x = \log_{10}$  converted data,  $y = \log_{10}$  converted standard length). These equations correspond to the scatter plots of figure 3... 56

**Table 2.** Ossification sequence reliability for each appendicular skeleton structure for 56 *Eusthenopteron foordi*. See explanations in the text for the definition and interpretation of the parameters. .... 57

## LISTE DES FIGURES

### Chapitre 1

**Figure 1.** Cross section in the nasal capsule region of *Eusthenopteron foordi*. **A.** Specimen MHNM 06-1001A (scan 8/36); **B.** Specimen MHNM 06-1045 (scan 8/16); **C.** Specimen RM 14234 (scan 102/110). Left column: Computed Tomography. Right column: Interpretation of the CT scan; black = bone, dark grey = ethmosphenoid, light grey = teeth. Abbreviations, **a.Te.:** anterior tectal, **ch.:** choana, **dml.p.:** dermintermedial process, **Dpl.:** dermopalatine, **Dt.:** dentary, **Ecpt.:** ectopterygoid, **Enpt.:** entopterygoid, **Ethm.:** ethmosphenoid, **f.:** fang, **Gul.:** gular plate, **ioc:** infraorbital canal, **l.Te:** lateral tectal, **m.cav.:** mouth cavity, **Mx.:** maxillary, **n.caps.:** nasal capsule, **n.op.:** nasal opening, **plp.cav.:** pulp cavity, **Pmx.:** premaxillary, **Pr.:** postrostral, **Psph.:** parasphenoid, **soc:** supraorbital canal, **Vo.:** vomer, **vo.f.:** vomerine fang. ....25

**Figure 2.** *Eusthenopteron foordi*, specimen MHNM 06-719. **A.** Ventral view of the palate; **B.** Close-up of the choana area; **C.** Camera-lucida drawing of the specimen. Scale bars : 1 cm. 1, 2 and 3 identify facets on the head of the dermopalatine. **Dpl.:** dermopalatine, **Ecpt.:** ectopterygoid, **Enpt.:** entopterygoid, **Mx.:** maxillary, **Psph.:** parasphenoid, **Vo.:** vomer, **vo.f.:** vomerine fang.....27

**Figure 3.** *Eusthenopteron foordi*, specimen MHNM 06-220. Ventral view of the palate. Scale bar ; 1 cm. **ch.:** choana, **Dpl.:** dermopalatine, **Enpt.:** entopterygoid, **Mx.:** maxillary, **Pmx.:** premaxillary, **Psph.:** parasphenoid, **Vo.:** vomer, **vo.f.:** vomerine fang.....28

**Figure 4.** Strict consensus trees obtained from previously published matrices. Trees obtained from: **A.** Cloutier & Ahlberg (1996); **B.** Zhu & Schultze (1997); **C.** Zhu & Schultze (2001); **D.** Johanson & Ahlberg (2001) matrices. 1 identifies appearance of the choana character, 0 identifies reversal of this character. Trees from original matrices are numbered on the right side of the branches, whereas trees from modified matrices (choana considered absent in *Eusthenopteron*) are numbered on their left side. **C** and **D** only have one tree because the topology remained the same after the matrix modification. Trees **B** and **D** show double appearance and/or reversal because it was not possible to know if the authors used “ACCTRAN” or “DELTRAN” options.....29

## Chapitre 2

**Figure 1.** Scatter diagram of standard length (mm) plotted against distance (mm) between insertion points of fins in *Eusthenopteron foordi*. The lower regression line ( $\square$ ) corresponds to the distance between insertion points of the first and second dorsal fins (D1-D2); the upper regression line ( $\circ$ ) corresponds to the distance between the insertion point of the second dorsal fin and the insertion point of the epichordal lobe of the caudal fin (D2-C). Data were obtained from Thomson and Hahn (1968), Schultze (1984), and original measurements.....70

**Figure 2.** Sequence of ossification of *Eusthenopteron foordi* for the pectoral, pelvic, dorsal and anal fins. Observed skeletal elements (dark rectangles) are recorded for 65 specimens. For each specimen, the standard length (S.L.) is given; a star indicates an estimated length according to the formulas given in the text. The light grey areas correspond to missing

parts owing to partial preservation of fossils. A and B designate part and counterpart of a specimen. **Bas.:** basal plate; **Clei.:** cleithrum; **Fem.:** femur; **Fib.:** fibula; **Hum.:** humerus;

**R1, R2 and R3:** first, second and third radial in an anterior to posterior position;

**Rad/Rads.:** radial/radials; **Scut.:** basal scutes.....71

**Figure 3.** Scatter diagrams of body measurements (mm) versus standard length (mm) in *Eusthenopteron foordi*. **A**, Distance from posterior margin of the operculum to the insertion of the first dorsal fin; **B**, distance from posterior margin of the operculum to the insertion of the second dorsal fin; **C**, distance from posterior margin of the operculum to the insertion of the pelvic fins; **D**, distance from posterior margin of the operculum to the insertion of the anal fin; **E**, distance from posterior margin of the operculum to the insertion of the epichordal lobe of the caudal fin; **F**, distance from posterior margin of the operculum to the insertion of the hypochordal lobe of the caudal fin. Regression lines are illustrated.....73

**Figure 4.** Small specimen of *Eusthenopteron foordi* (UL 265). Enlarged view of the pectoral girdle region, showing the first ossified branchial elements. **b.sc.:** basal scute; **Cbr.:** ceratobranchials; **Dt.:** dentary; **l.Ano.:** anocleithrum; **l.Cl.:** left cleithrum; **l.Cla.:** left clavicle; **l.l.Gu.:** left lateral gular plate; **Op.:** opercular; **pec.f.:** pectoral fin; **r.Cl.:** right cleithrum; **r.Cla.:** right clavicle; **r.l.Gu.:** right lateral gular plate; **sbm.:** submandibular; **Sc.:** scales. Scale bar equal 5 mm.....75

**Figure 5.** Schematic representation of the ossification of each fin in *Eusthenopteron foordi*. Stages are progressive from left to right. Solid lines correspond to fin rays, dark grey elements are endochondral bony structures and light grey elements are basal scutes. Arrows indicate direction of ossification.....76

- Figure 6.** Caudal region of *Eusthenopteron foordi*, specimen MHNM 06-59 (S.L. ca. 111 mm). Rod-shaped basal elements in both the second dorsal fin and the anal fin in early stage of development. **A. rad.:** anal fin radials; **b.pl.:** basal plate; **D2 rad.:** second dorsal fin radials; **H.sp.:** haemal spines; **N.sp.:** neural spines; **V.c.rad.:** ventral caudal radials. Scale bar equals 10 mm.....78
- Figure 7.** Sequence of ossification of *Eusthenopteron foordi* for the vertebral column and the caudal fin. Skeletal elements present in each of the 65 observed specimens, identified by their standard length (same order as in figure 2). The light grey shadowed areas are missing parts of the fossils. Legend :  Neural spines;  Haemal spines;  Intercentra;  Pleurocentra;  Caudal ventral radials.....79
- Figure 8.** Specimen of *Eusthenopteron foordi* (UL 95, S.L.: 59.9 mm). **A,** Complete specimen. **B,** Details of the anterior ventral radials of the caudal fin. Three of them show evidence of collapsing (longitudinal grooves) owing to taphonomic process. Scale bars equal 1 mm.....81
- Figure 9.** Three of the smallest specimens of *Eusthenopteron foordi*, showing the early ossification of the basal scutes. **A,** AMNH 7687A; **B,** AMNH 7650; **C,** UL 121A; **D,** enlargement of the anal fin region of specimen UL 121A. Scale bars equal 5 mm.....82
- Figure 10.** Anal fin of *Eusthenopteron foordi* showing the segmentation and branching of the lepidotrichia. Circles indicate branching. **A,** FMNH UC 2127 (S.L.: 102.3 mm); **B,** FMNH UF 45 (S.L.: ca. 252 mm). **b.Pl.:** basal plate; **ra.:** radial. Scale bars equal 5 mm .....83

**Figure 11.** Ontogenetic pathway of *Eusthenopteron foordi*. The cumulative number of ossified elements for 65 specimens is traced against the specimen standard length. Values 1 to 6 are rate of development expressed in terms of the mean number of new elements for each millimetre of growth (elements/mm) for each step and threshold.....84

## INTRODUCTION GÉNÉRALE

La paléontologie moderne ne se contente plus de livrer de simples descriptions anatomiques des organismes fossilisés qu'elle étudie. Elle arrive aujourd'hui, par des méthodes de pointe, à découvrir la façon dont vivaient ces êtres disparus, les distances phylogénétiques qui les séparent, la nature de l'habitat dans lequel ils évoluaient. Certaines espèces sont plus fréquemment trouvées (e.g., plusieurs espèces de trilobites), d'autres se voient accorder une grande importance dans l'histoire de la vie (e.g., l'*Archaeopteryx lithographica*), d'autres encore acquièrent une renommée souvent due à leurs impressionnantes caractéristiques physiques (e.g., le *Tyranosaurus rex*).

Le Québec aussi a son fossile « populaire ». Trouvé dans les falaises de Miguasha en Gaspésie, l'*Eusthenopteron foordi* Whiteaves 1881 est un poisson sarcoptérygien qui vivait il y a environ 370 millions d'années (Frasnien, Dévonien supérieur). Connu depuis plus de 125 ans, le nombre de spécimens récoltés dépasse aujourd'hui 2 200 (Parent et Cloutier, 1996) et les publications sur son sujet se chiffrent à près de 200 (sans compter toutes celles qui ne font que mentionner l'espèce; Cloutier, 1996). Il est devenu, notamment grâce aux travaux de Jarvik (1942, 1980), l'un des vertébrés fossiles les mieux connus et décrits et il fut élevé assez tôt au rang de taxon clé dans la transition menant des « poissons » aux tétrapodes (Cope, 1892), principalement à cause des particularités anatomiques de ses nageoires paires qui rappellent les membres des tétrapodes.

Dès lors, à cause de son statut « hybride » entre aquatique et terrestre, une relative importance fut accordée à l'étude du museau de l'*Eusthenopteron foordi* et de ses conduits

nasaux (Jarvik, 1942; Panchen, 1967) afin de déterminer à quel point il se rapprochait phylogénétiquement des tétrapodes. Ici, la structure qui a le plus attiré l'attention est la choane, i.e. l'orifice dans le palais de la majorité des rhipidistiens qui relie la cavité buccale à la cavité nasale et permet la respiration aérienne lorsque la bouche est fermée. Des choanes étaient considérées présentes chez *E. foordi* jusqu'en 1981, date à laquelle Rosen et al. (1981) ont publié une nouvelle description de l'animal dans laquelle les orifices palataux ne sont pas considérés comme des choanes fonctionnelles. Les années suivantes ont vu la publication de nombreuses critiques, aussi bien de ceux qui considèrent la choane présente chez *E. foordi* (Jarvik, 1981; Holmes, 1985; Panchen et Smithson, 1987; Schultze, 1987, 1991), que de ceux qui n'y croient pas (Chang, 1991; Forey et al., 1991). Mais aucun de ces articles n'est le résultat de travaux d'observation sur de nouveaux spécimens, tous les auteurs se contentant de citer des travaux antérieurs. Le premier chapitre du présent mémoire est le fruit de l'étude de nouveaux spécimens d'*Eusthenopteron foordi* par des méthodes inédites et propose de mettre un terme à ce débat vieux de 24 ans.

Mais les fossiles ne permettent pas seulement des études anatomiques. Des réalités plus dynamiques, comme le développement et la croissance, peuvent aussi être investiguées. Depuis une trentaine d'années, l'étude du développement des vertébrés dans une perspective phylogénique a pris une grande ampleur dans les laboratoires d'évolution (Gilbert et al., 1996; Holland, 1999; Goodman et Coughlin, 2000; Arthur, 2002). Les différentes espèces ne sont plus comparées entre elles seulement selon leurs caractéristiques morphologiques et anatomiques, mais aussi selon les ressemblances et différences entre leurs développements respectifs, aussi appelés leurs ontogénies. Retracer les séquences

ontogénétiques d'un animal donné permet (Mabee et Trendler, 1996; Smith, 2001; Jeffery et al., 2002 a,b; Grunbaüm, 2004) (a) d'estimer sa proximité phylogénétique relative avec les autres espèces dont on connaît aussi l'ontogénie, (b) de voir les nouveautés acquises dans le développement des espèces durant l'évolution, et (c) d'utiliser des séquences ontogénétiques détaillées comme caractères pouvant être codés dans l'élaboration d'arbres phylogénétiques. Cette branche relativement récente des sciences de la vie, appelée biologie évolutive du développement, ou évo-dévo, permet entre autres d'affiner les liens phylogénétiques entre espèces lors de reconstructions cladistiques.

L'établissement des patrons de développement, appliqué surtout aux espèces vivantes (Mabee, 1993, 2000; Cabbage et Mabee, 1996; Mabee et Trendler, 1996; Grunbaüm et al., 2003), est parfois tenté chez des espèces fossiles (Cote et al., 2002; Chipman et Tchernov, 2002). Il faut pour cela avoir accès à suffisamment d'individus d'âges différents conservés dans un excellent état afin de voir les structures présentes à tous, ou du moins à plusieurs stades de croissance. Les spécimens d'*Eusthenopteron foordi* trouvés dans la Formation d'Escuminac (Miguasha) étant relativement nombreux et de toutes tailles, ils permettent l'étude de la croissance chez ce poisson. Les résultats des observations sur un échantillon de 65 spécimens, de tailles comprises entre 27 et 270 mm, sont présentés au deuxième chapitre de ce mémoire. Il a été possible de reconstruire une trajectoire ontogénétique pour l'espèce et celle-ci pourra servir de comparatif pour les éventuelles études du même type chez d'autres espèces.

Ensemble, ces deux chapitres constituent un complément d'information sur cette espèce remarquable qui laisse apparaître de nouvelles possibilités d'investigation à chaque

nouvelle étude. Le premier prétend régler une controverse, et le suivant apporte de nouvelles données dans un domaine en plein essor, la biologie évolutive du développement.

## RÉFÉRENCES

- Arthur, W. 2002. The emerging conceptual framework of evolutionary developmental biology. *Nature* 415:757-764.
- Cope, E. D. 1892. On the phylogeny of the Vertebrata. *Proceedings of the American Philosophical Society* 30:278-281.
- Cubbage, C. C. and P. M. Mabee. 1996. Development of the cranium and paired fins in the zebrafish *Danio rerio* (Ostariophysi, Cyprinidae). *Journal of Morphology* 229:121-160.
- Forey, P. L., B. G. Gardiner and C. Patterson 1991. The lungfish, the coelacanth, and the cow revisited. pp. 145-172 in H.-P. Schultze and L. Trueb (eds), *Origins of the major groups of tetrapods: controversies and consensus*. Cornell University Press, Ithaca.
- Gilbert, S. F., J. M. Opitz and R. A. Raff 1996. Resynthesizing evolutionary and developmental biology. *Developmental Biology* 173:357-372.
- Goodman, C. S. and B. C. Coughlin. 2000. The evolution of evo-devo biology. *Proceedings of the National Academy of Sciences* 97(9):4424-4425.
- Grünbaum, T. 2004. Étude des séquences de chondrification et d'ossification durant le développement du système caudal chez cinq espèces de poissons cypriniformes :

- interaction entre l'ontogénie et la phylogénie. Mémoire de maîtrise. Université du Québec, Rimouski.
- Holland, P. W. H. 1999. The future of evolutionary developmental biology. *Nature* 402:C41-C44.
- Jeffery, J. E., O. R. P. Bininda-Emonds, M. I. Coates and M. K. Richardson. 2002a. Analyzing evolutionary patterns in amniote embryonic development. *Evolution and Development* 4:292-302.
- Jeffery, J. E., M. K. Richardson, M. I. Coates and O. R. P. Bininda-Emonds. 2002b. Analyzing developmental sequences within a phylogenetic framework. *Systematic Biology* 51:478-491.
- Mabee, P. M. 1993. Phylogenetic interpretation of ontogenetic change: sorting out the actual and artefactual in an empirical case study of centrarchid fishes. *Zoological Journal of the Linnean Society* 107:175-291.
- Mabee, P. M. 2000. Developmental data and phylogenetic systematics: evolution of the vertebrate limb. *American Zoology* 40:789-800.
- Smith, K. K. 2001. Heterochrony revisited: the evolution of developmental sequences. *Biological Journal of the Linnean Society* 73:169-186.

## REMERCIEMENTS

Ça porte bien son nom, une maîtrise... On y apprend la maîtrise de soi et de ses envies de faire autre chose...

Ces trois années passées à Rimouski m'ont bien servies et m'ont permis de me connaître, de savoir ce que j'aimais et ce que j'aimais moins. L'essentiel de mes remerciements ira à Richard Cloutier, mon directeur de recherche. Il a eu la difficile tâche de piloter un étudiant pour qui les études de maîtrise étaient vues comme un projet parmi de nombreux autres. Malgré mon inconstance, malgré mes pannes de motivations, malgré nos déceptions réciproques, il a gardé le cap, a continué à me pousser sans cesse, en dépit des orages auxquels il avait lui-même à faire face. Le présent mémoire est le fruit de cette persévérance: sans l'énergie de Richard, le projet se serait probablement éteint assez rapidement. Le résultat final est à l'honneur de cet homme de grandes qualités.

Les quelques centaines d'heures passées dans les sous-sols de musées à dessiner des fossiles ou à jongler avec les bases de données pour en obtenir des résultats cohérents en valaient bien la peine finalement. Avec le recul, je suis fier de présenter un rapport étoffé et rigoureux, résultat d'un important travail d'observation et d'acquisition de données. C'est souvent en se retournant qu'on peut contempler l'ampleur du chemin parcouru. Et celui que je peux voir a été tortueux, mais gratifiant.

Je m'en voudrais de passer sous silence l'apport de Claudette et Gaston, mes parents, l'homme et la femme de ma vie, qui oeuvrent sans relâche en coulisse pour me supporter et m'aider dans tous les projets que j'entreprends, aussi farfelus soient-ils. Merci pour cet amour inconditionnel.

## CHAPITRE 1

**New data and new methods on an old problem: the choana revisited.**

**Joël Leblanc and Richard Cloutier**

Laboratoire de Biologie évolutive, Université du Québec à Rimouski,

300 allée des Ursulines, Rimouski, Québec, G5L 3A1, Canada

richard\_cloutier@uqar.qc.ca

RH : LEBLANC AND CLOUTIER - CHOANA OF *EUSTHENOPTERON*

## ABSTRACT

Interrelationships among sarcopterygians and among osteolepiforms more specifically have been the focus of numerous analyses and debates during the past 20 years. Differences among phylogenetic hypotheses resulted from (1) different methodological approaches, (2) the selection of taxa, and (3) the selection and homology of characters. In numerous sarcopterygian phylogenies, the Late Devonian tristichopterid *Eusthenopteron foordi* (Escuminac Formation, Miguasha, eastern Canada) was selected as the sole representative of osteolepiforms. The presence of a choana - a character considered by different authors as a "key" character in relation to the origin of tetrapods - in *E. foordi* has been questioned frequently. Various critics and scenarios have been suggested to negate the presence of a choana in this species; the palatal opening has been interpreted as (1) part of a mobile joint between the snout and the cheek/palate unit, (2) a duct for nerves and blood vessels, (3) a pit to accommodate a coronoid fang during mouth occlusion, and (4) an artefact owing to mechanical or acid preparation of the specimens. New material of *E. foordi* has been prepared in order to display the palatal anatomy. In addition, non-invasive CT-scans have been performed on three-dimensional unprepared specimens. The presence of a choana in *E. foordi* is confirmed. However, the size of the palatal opening and the relative position of coronoid fangs differ from previous interpretations. Independently from the presence of a choana, the phylogenetic coding of *E. foordi* (with or without a choana) and the deletion or addition of the choanal character have little impact on the length of the trees, number of equally most parsimonious trees, and the resolution of sarcopterygian and osteolepiform interrelationships.

## RÉSUMÉ

Les relations phylogénétiques entre les sarcoptérygiens, et plus spécifiquement entre ostéolépiformes, ont été l'objet de nombreuses analyses et débats au cours des 20 dernières années. Les différences entre hypothèses phylogénétiques sont dues à (1) des approches méthodologiques différentes, (2) le choix des taxons et (3) le choix et l'homologie des caractères. Dans plusieurs phylogénies des sarcoptérygiens, le tristichoptéride *Eusthenopteron foordi* du Dévonien supérieur (Formation d'Escuminac, Miguasha, est du Canada), a été utilisé comme unique représentant des ostéolépiformes. La présence d'une choane – un caractère considéré par différents auteurs comme un caractère « clé » en ce qui concerne l'origine des tétrapodes – chez *E. foordi* a été souvent mise en doute. Des critiques et scénarios variés ont été avancés pour réfuter la présence d'une choane chez cette espèce, l'ouverture palatale étant alors interprétée comme (1) une partie d'une articulation mobile entre le museau et l'ensemble palais-joue, (2) un conduit laissant passage à des nerfs et des vaisseaux sanguins, (3) une fossette pouvant recevoir un croc coronoïdien lors de l'occlusion buccale et (4) un artefact dû à la préparation des spécimens, à l'acide ou par des procédés mécaniques. De nouveaux spécimens d'*E. foordi* ont été préparés afin de révéler l'anatomie du palais. De plus, des tomographies assistées par ordinateur ont été réalisées sur des spécimens tridimensionnels non préparés. La présence d'une choane chez *E. foordi* est maintenant confirmée. Toutefois, les dimensions de l'ouverture palatale et la position relative des crocs coronoïdiens diffèrent des interprétations antérieures. Indépendamment de la présence d'une choane, le codage (avec ou sans choane) et le retrait ou l'ajout du caractère choane dans les analyses

phylogénétiques n'a que peu d'influence sur le nombre d'arbres également parcimonieux, sur leur longueur et sur la résolution des relations entre sarcoptérygiens et entre ostéolépiformes.

## INTRODUCTION

For the past 20 years, numerous controversies have challenged sarcopterygian systematics. Reasons for these inconsistencies are related to the material itself (e.g., rarity of specimens, incompleteness of fossils, poor fossil preservation) or to methodological considerations (e.g., different approaches, selection of taxa, selection and homology of characters). Until recently, hypotheses of sarcopterygian interrelationships greatly vary among authors (see Schultze 1991). The proposed tetrapod sister-group, for instance, was successively interpreted as the dipnoans (Rosen et al. 1981), osteolepiforms (Schultze 1987, Panchen and Smithson 1987) and elpistostegalians (Cloutier and Ahlberg 1996, Zhu and Schultze 2001).

Most recent phylogenetic analyses of sarcopterygians utilize large and diversified data matrices including up to 216 characters (Zhu and Schultze 2001). Among these characters, the presence of a choana has generated special interest because of its functional interpretation related to the terrestrialization of vertebrates (Jarvik 1942, Panchen 1967, Jurgens 1971). According to Schultze (1987), the choana can be defined in two complementary ways: (1) an opening in the palate surrounded primitively by four dermal bones - the premaxilla, maxilla, vomer and palatine - (morphological definition), and (2) a palatal opening for a pathway beginning with one opening outside the mouth, the external naris (in tetrapods, the pathway for air, with the mouth closed; functional definition).

Characters related to the choana have been used to diagnose different taxa by different authors. Subtle differences concern the character definition itself as well as the taxonomic definition of the clades. Rosen et al. (1981, char. 42) considered the presence of

a choana as a synapomorphy of Dipnoi plus Tetrapoda, a clade that they referred to as the Choanata. In opposition, Schultze (1987, char. 42) considered the presence of the choana as a synapomorphy shared by Osteolepiformes, Elpistostegalia and Tetrapoda, a clade he also called the Choanata, but which excludes the Dipnoi. Vorobyeva and Schultze (1991, char. 24) used the presence of a “choana between premaxilla, maxilla, vomer and dermopalatine” as a synapomorphy of the Choanata (i.e., [Osteolepiformes + Rhizodontida + [Elpistostegalia + Tetrapoda]] ). Cloutier and Ahlberg (1996, char. 48) considered the presence of a “palatal opening (choana) surrounded by premaxilla, maxilla, dermopalatine, and vomer” as an homoplasy occurring (1) in Porolepiformes and (2) in Rhipidistia. The usage of Rhipidistia by Cloutier and Ahlberg (1996) includes the Dipnoiformes; however, this clade is characterized by a reversal for the choana character. In Zhu and Schultze’s (2001; char. 113) analysis, the presence of a “palatal opening surrounded by premaxilla, maxilla, dermopalatine and vomer” is homoplastic occurring in (1) the clade [*Holoptychius* + *Glyptolepis*] and (2) the Osteolepidida (i.e., [Osteolepiformes + [*Eusthenopteron* + [Elpistostegalia + Tetrapoda] ] ]). In contrast to Cloutier and Ahlberg (1996) and Zhu and Schultze (2001), Clement (2001) mentioned that a choana is absent from porolepiforms, a view originally expressed by Jarvik (1972). Zhu and Ahlberg (2004) recently resolved a debate concerning the origin of the choana and proposed a reconstruction of *Kenichthys campbelli* in which a transitional state between the posterior naris of bony fishes and the palatal choana of tetrapodomorphs is visible, breaking down the suture between the premaxilla and maxilla.

As it can be seen, no general consensus emerges from past analyses. Independently from the phylogenetic hypotheses, the occurrence of a choana in *Eusthenopteron foordi* is still debated. Bryant (1919), Stensiö (1921, 1922), Watson (1926), Holmgren and Stensiö (1936) and Jarvik (1937, 1942, 1980) described a choana in *E. foordi* (“internal nares” of Bryant, “fenestra exochoanalis” of Jarvik). But in 1981, Rosen et al. published a new description of *E. foordi* based on four specimens from The Natural History Museum, in London (UK), one of them having been prepared with acetic acid (BMNH P. 60310). Their reconstruction differs in many points from that of Jarvik (1942), particularly by a much smaller size of the palatal opening. They argued that the foramen described as a choana by Jarvik (1942) was not such a structure according to the functional definition and they suggested three hypotheses for its use: (1) a part of a mobile joint between the snout and the cheek/palate unit, (2) a duct for nerves and blood vessels, and (3) a pit to accommodate a coronoid fang during mouth occlusion. Furthermore, Chang (1991, p.11) reviewed Jarvik’s interpretation of the choana in two specimens (SMNH P.341 and P.222) and suggested that “the only “rhpidistian” that might have possessed a passage between the nasal and mouth cavities is *Eusthenopteron foordi*, but as Rosen et al. (1981) pointed out, its presence is questionable.” In fact, she favoured Rosen et al.’s interpretation of a mobile articulation between the palatoquadrate-cheek unit and the snout.

Since the publication of Rosen et al. (1981), numerous critics have been published to demonstrate the presence of a choana in osteolepiforms and its absence in dipnoans (Schultze 1981, 1987, 1991, Jarvik 1981, Campbell and Barwick 1984, Holmes 1985, Panchen and Smithson 1987), but new material of *E. foordi* has never been prepared and

studied. The number of specimens of *E. foordi* now exceeds 2100 specimens (Parent and Cloutier 1996, Cloutier et al. 1997) and new specimens are discovered every year by the personnel of the Parc National de Miguasha. Evidently, a small number of specimens display choanal characteristics. Previous methods for examination of fossils, such as serial grinding for Jarvik (1942) or acid preparation for Rosen et al. (1981), have been criticized for their potential destructive effects and the possibility of “generating” artificial choanas. Here we report the first results of examination of new specimens since 1981, using CT scan on four three-dimensional skulls, a non-invasive method to study internal morphology.

## **MATERIAL AND METHODS**

Three specimens of *Eusthenopteron foordi* (MHNM 06-1045, 06-1001A, RM 14234) and one specimen of the elpistostegalian *Elpistostege watsoni* (MHNM 06-538) were scanned with a medical CT scan. Two specimens of *E. foordi* (MHNM 06-719, 06-220) offering direct ventral view of the palate were also used. MHNM specimens were scanned with a Picker Scanner with the following parameters: 130 kV, 125 mA, slice thickness 2.0 mm and interslice spacing 2.0 mm. Specimen RM 14234 was scanned with a Somatom Volume Access with the following parameters: 140 kV, 140 mA, slice thickness 0.3 mm and interslice spacing 0.5 mm. The images were processed with Osiris 4.15 (Medical Imaging Software). Corrected measures were taken on cross sections after inclination of images with Corel PHOTO-PAINT 8.369 software to compensate for specimen deformation.

In the text, head length is as defined by Schultze (1984, measurement no. 5) and the snout height is the vertical measure between the ventral margin of the upper jaw (premaxilla or maxilla, depending on which level) and the top of the skull at the same level.

Phylogenetic analyses were performed using PAUP\* 4.0b10 (SWOFFORD 2002). Four different matrices were used (Cloutier and Ahlberg 1996, Zhu and Schultze 1997, Johanson and Ahlberg 2001, Zhu and Schultze 2001).

**Institution abbreviations:** BMNH, The Natural History Museum, London, UK; MHNM, Musée d'Histoire Naturelle de Miguasha, Québec, Canada; RM, Redpath Museum, McGill University, Montréal, Québec, Canada.

## RESULTS

The skull of specimen RM 14234 (length of head: 13,5 cm) is only slightly deformed. The specimen is compressed laterally and the left side is slightly higher than the right side, but this was corrected by computerized images processing.

Only the left nasal area of specimen MHNM 06-1045 (length of head: 14,5 cm) is well preserved. The right nasal capsule is incomplete because the right mandible and maxilla are crushed against the right side elements. The overall shape of the snout itself is perfectly preserved, without apparent deformation. The resolution of the cross sections (2 mm thickness) and the large interval between each of them (2 mm) render the interpretation less precise.

Specimen MHNM 06-1001A is one of the largest known three-dimensional skulls of *E. foordi* (length of head: 28,0 cm). Numerous skull roofing and cheek bones are missing; nevertheless, the skull is in an excellent three-dimensional shape. As for MHNM 06-1045, cross sections were done at every 2 mm and each slice is 2 mm thick. Nasal regions are visible on both sides of the head.

The resolution of CT cross sections (fig. 1) on all three specimens allow us to describe the general morphology of the nasal capsule without preparing specimens mechanically or with acid. On both sides of the head, the anterior external naris is surrounded dorsally by the anterior tectal and ventrally by the lateral tectal. The maximum relative height of the external naris varies among individuals; 7,6% (MHNM 06-1001A), 11,3% (RM 14234) and 16,9% (MHNM 06-1045) of the snout height. It is nearly symmetrical on specimens where both openings are visible.

The naris outline itself is pear-shaped, with the narrow part pointing toward the orbit. The external naris on MHNM 06-1045 reveals that, as in Bjerring's (1989: Fig. 2E, p.77) illustrations, the inner surface of the canal (upper surface of the dermintermedial process) is smooth (in opposition with the condition in *Gogonasmus andrewsae*, where the nasal opening is ornamented with denticles, Long et al. 1997). The canal leading from the nasal opening is ornamented with denticles, Long et al. 1997). The canal leading from the external nostril to the nasal cavity is only visible and measurable on specimen RM 14234. It has a maximum depth of 1,8 mm and the snout width at this level is 21,7 mm. From the naris, the canal is oriented medially and perpendicular to mid-body plan. The canal corresponds solely to the thickness of the anterior tectal dorsally. The canal enters the capsule antero-laterally in the upper part of the capsule.

The nasal capsule lies adjacent to the ethmoidal wall. The paired capsules occupy approximately one third of the snout width and are separated widely by the ethmosphenoid. Inside the capsule, the dermintermedial process extends anteroposteriorly along the lateral wall of the nasal capsule; it divides incompletely the nasal capsule into dorsal and ventral chambers. The process never extends more than half of the capsule width.

Most of the nasal capsule floor is open, leading to the mouth cavity. From the opened floor of the nasal cavity to the palate, the radiographic sections reveal a passage formed by the ventral tooth-bearing laminae of the premaxilla and by the vomer; this passage corresponds to the choana. More posteriorly, this choana is delimited by the maxilla and the dermopalatine. The depth of the choana is 7,5 mm for a 17,1-mm high snout in RM 14234 (relative depth of 43,9%), 9,8 mm for a 22,5 mm-high snout in MHNM 06-1045 (43,6%) and 12,6 mm for a 27,7 mm-high snout in MHNM 06-1001A (45,0%). The elongated choana extends posteriorly from the level of the posterior margin of the external nasal opening to the level of the first dermopalatine teeth. In palatal view, the choana itself is 2,7 mm wide at a level where the palate is 20,6 mm wide in RM 14234 (relative width of 13,1%), 3,6 mm in a 29,7 mm-wide snout in MHNM 06-1045 (12,0%) and 6,0 mm in a 43,3 mm-wide snout in MHNM 06-1001A (13,9%). Relative dimensions of the structures associated with the nasal capsule are summarized in Table 1.

On the left side of specimen RM 14234, the dermopalatine is displaced, pointing upward in the nasal capsule and its extremity almost touches the external naris.

Specimen MHNM 06-1001A is preserved with the mandible in natural occluding position. Radiographic sections reveal that the tip of the anteriormost coronoid fang

occludes directly on the flat surface of the dermopalatine, and does not fit into a pit as suggested by the third hypothesis of Rosen et al. (1981).

Bones surrounding the choana are visible in specimens MHNM 06-719 (Fig. 2) and 06-220 (Fig. 3). On both specimens, only structures of the right side of the palate are clearly visible because of the displacement of left maxilla. The choana is surrounded by four bones: anterolaterally by the posterior part of the premaxilla, posterolaterally by the anterior part of the maxilla, anteriorly and medially by the vomer and posteriorly by the anterior part of the dermopalatine.

The anterior process of the dermopalatine of specimen MHNM 06-719 (Fig. 2B) bears three articular facets, all pointing more or less directly toward the lateroposterior margin of the vomer. This situation is also represented in Rosen et al. (1981) reconstruction, but the facets of specimen MHNM 06-719 were fairly different both in position and in orientation from those of Rosen et al. The largest facet (1, Fig. 2B) is pointing forward and its tip disappears dorsally to the vomer in palatal view. The two other facets lie ventral and dorsal to the first one. The most ventral one (2, Fig. 2B) is facing dorsally but is not articulated with the vomer. The most dorsal facet (3, Fig. 2B) is facing ventrally but is posteriorly situated too far to articulate with the vomer's margin. This last facet would actually touch and skirt the circular base of the first dermopalatine fang if it was still in place.

### ***Phylogenetic analyses***

In order to investigate the importance of the choana character in terms of phylogenetic resolutions, previously published data matrices were reanalysed. Four data matrices have been studied: Cloutier and Ahlberg (1996: 140 characters and 33 taxa), Zhu and Schultze (1997: 140 characters and 33 taxa; 2001: 216 characters and 33 taxa) and Johanson and Ahlberg (2001: 99 characters and 30 taxa). The data matrices used by Cloutier and Ahlberg (1996) and Zhu and Schultze (1997) were created to study sarcopterygian interrelationships, whereas the Zhu and Schultze (2001) matrix was designed to address basal osteichthyan interrelationships. Johanson and Ahlberg (2001) constructed their matrix to investigate osteolepiform interrelationships. *Eusthenopteron foordi* was included in these four data matrices, in each of these analyses, a choana was also considered to be present. For each one of the data matrices, three analyses were performed reconsidering the coding of *E. foordi*: (1) one analysis in which a choana was considered absent (plesiomorphic) in *E. foordi*, (2) one analysis corresponding to our observation in which a choana is present in *E. foordi* (apomorphic) and (3) one analysis in which the choana character is deleted. The analyses were performed with PAUP 4.0b10\* (Swofford 2002), using the heuristic search, all characters being entered unordered and unweighted. Tree length and number of equally parsimonious trees might differ from the original publications because some authors choose to order some characters (Johanson and Ahlberg 2001, Zhu and Schultze 2001) or used different versions of PAUP. Tree statistics are summarized in Table 2.

The data matrix previously published by Cloutier and Ahlberg (1996) gave 54 equally parsimonious trees at 278 steps (277 steps in the original paper). The deletion of the choana character (char. 48) gave 54 trees at 276 steps and the strict consensus tree (Fig 4A) remains unchanged. This difference of two steps is explained by the fact that, in the original tree, the choana occurs once, at the node [Onychodontida + Rhipidistia], but is reversed in Dipnoiformes. In the new analysis, these two steps disappear. Considering a choana absent in *E. foordi*, 18 trees were found at 278 steps. In the strict consensus tree, the original Tetrapodomorpha trichotomy is resolved; *E. foordi* is considered the sister-group of the remaining osteolepiforms (Fig. 4A). The choana character appears independently at the base of the Osteolepidida excluding *E. foordi* and at the base of the Porolepiformes. The choana character is thus responsible for two steps in this new cladogram, explaining the fact that the number of steps is similar to the original number of trees (278). The remaining part of the topology remains unchanged.

Analyses performed on Zhu and Schultze's (1997) data matrix give results similar to those obtained after manipulations on Cloutier and Ahlberg's (1996) matrix; most of the data matrix is identical in both papers. A total of 54 trees at 274 steps were obtained when removing the choana character (char. 48), whereas the original analysis provided 54 trees at 276 steps. The difference of two steps corresponds to the appearance of the choana at the node including *Youngolepis* plus more derived taxa (ACCTTRAN) or the porolepiforms clade plus more derived taxa (DELTRAN), and its reversal at the base of [[*Diplocercides kaeseri* + *D. heiligenstockiensis*] + *Allenpyterus*] (DELTRAN) or [actinistians + onychodonts] (ACCTTRAN) clades (Fig. 4B). Uncertainties are due to the impossibility to

know if the authors used ACCTRAN or DELTRAN option in their original analysis. We obtain 18 trees at 276 steps when considering the choana absent for *E. foordi*. The Tetrapodomorpha trichotomy is resolved here the same way it was in Cloutier and Ahlberg (1996) and the main topology remains unaltered (fig. 4B). We still have two steps for the choana character, because it appears independently in [*Holoptychius* + *Porolepis*] or in porolepiforms and osteolepiforms (excluding *E. foordi*).

With Zhu and Schultze's (2001) matrix, the analysis without changing the data matrix gave 60 trees at 461 steps [45 trees at 464 steps in the original paper – the presence of 15 additional three step shorter trees is because all characters were analysed unordered in contrast with Zhu and Schultze (2001)]. Removing the choana character (char. 113) reduces the number of steps to 459, whereas the number of trees remains the same. These two steps correspond to the presence of a choana in crossopterygians (sensu Zhu and Schultze) above *Powichthys* and a reversal in actinistians or [actinistians + onychodonts]. A total of 60 trees at 462 steps were found when *E. foordi* was considered as lacking a choana. The choana character is responsible for three steps in this new cladogram: the two former ones and another reversal for *E. foordi*. In both cases, the topology remains unchanged (Fig.4C).

Johanson and Ahlberg's (2001) matrix gives six equally parsimonious trees at 193 steps (six trees at 197 steps in the original paper). With the choana character (char. 28) omitted, we obtain six trees at 192 steps with no effect on the topology. The difference of one step corresponds to the appearance of a choana at the node Tetrapodomorpha including *Kenichthys* or not, depending on the option used, DELTRAN or ACCTRAN. With the

choana character coded 0 for *E. foordi*, we obtain six trees at 194 steps with no effect on the topology (Fig. 4D). The two steps correspond to the appearance of the choana still at the base of Tetrapodomorpha (with or without *Kenichthys*) at the same location, but a reversal is added for *Eusthenopteron*. In this matrix, Johanson and Ahlberg (2001) considered the choana as absent in *Glyptolepis*, in contrast to Cloutier and Ahlberg (1996) and Zhu and Schultze (1997, 2001).

## DISCUSSION

Rosen et al. (1981) argued that the structure long considered as a choana in *Eusthenopteron foordi* by numerous authors was not compatible with the functional definition of a choana, arguing that the canal leading from the mouth cavity to the nasal capsule was too small and obstructed. They suggested three hypotheses for the interpretation of the palatal opening: (1) part of a mobile joint between the snout and the cheek/palate unit, (2) a duct for nerves and associated blood vessels, or (3) a pit to accommodate a coronoid fang during mouth occlusion. Chang (1991) favoured Rosen et al.'s mobile articulation hypothesis, also suggesting that palatal bones positions and dimensions were greatly variable among specimens of *E. foordi*. However, this suggested variation has never been described.

Radiographic sections on the three specimens of *Eusthenopteron foordi* clearly reveal a non-obstructed duct leading from the nasal capsule to the mouth cavity on both sides of the head. The relative maximum width of the choana for each specimen was

measured directly on the radiographic section on which the choana was the widest. The relative maximum size of the choana varies from 12,0% to 13,9% of the snout width.

The observed relative width of the choana agrees with Jarvik's (1942) reconstruction (12 to 15%), and consequently differs from Rosen et al. (1981) one (5%). The position of the coronoid fangs during occlusion reveals that none of them was in the choana when the mouth was closed, thus refuting the third alternative hypothesis of Rosen et al. (1981) proposed to explain the presence of that orifice in the palate.

Except for the relative proportions of the external nostril, the anatomy of the nasal region also shows relatively constant proportions among the three specimens (Table 1). This consistency among the measurements challenges Chang's (1991) proposition that the anatomy could be greatly variable among specimens.

Our description of the main palatal bones corresponds to the classic reconstructions of *Eusthenopteron foordi* (Bryant 1919, Jarvik 1937, 1942). However, the anterior end of the dermopalatine bears three articular facets, two of them being too far to the latero-posterior margin of the vomer to articulate with it, as described by Rosen et al. (1981). Our observed specimens do not seem to have any displacement of the palatal bones, revealing a wide open choana like in Jarvik's reconstructions and a dermopalatine wearing three articular facets at its head, like in Rosen et al.'s reconstruction.

The present results, those of Clement (2001) (confirming the absence of choana in porolepiforms), and those of Zhu and Ahlberg (2004) (proposing a solution to the debate on the origin of the choana and stating that the dipnoan "choana" is not homologous to that of

tetrapodomorphs), will clarify the long-time uncertainty about the presence/absence of choanal aperture in some clades.

Despite this, our phylogenetic analyses of previously published matrices (Cloutier and Ahlberg 1996, Zhu and Schultze 1997, Johanson and Ahlberg 2001, Zhu and Schultze 2001, table 2) shows that the choana character does not have the phylogenetic importance that is often given to it. Deletion of the character and differential determination of that character state for *Eusthenopteron foordi* (absent or present) have little influence if any on the final topology of sarcopterygian relationships. In comparison with pre-Hennigian hypotheses to identify tetrapod ancestry, modern analyses take into account an important number of characters [from 99 (Johanson and Ahlberg 2001) to 216 characters (Zhu and Schultze 2001)]. When all of them are equally weighted, most of them don't have enough importance to significantly change cladograms configuration all alone (principle of total evidence). Despite its probable evolutionary importance, the choana is no more than a character among others in phylogenetic studies.

## **ACKNOWLEDGEMENTS**

We wish to thank André Chagnon and Bernard Long from the Institut National de la Recherche Scientifique (Québec City, Canada) and Michel Bovo from Centre Hospitalier Régional Restigouche (Campbellton, New Brunswick, Canada) for CT Scan expertise. Robert L. Carroll (McGill University) and Marius Arsenault (Musée d'Histoire Naturelle de Miguasha) loaned the specimens. Robert Chabot shot, developed and printed the pictures. This research was supported by a NSERC research grant to Richard Cloutier

(238612) and by the Fondation Gérard D. Lévesque. Jean Ferron and Hans Larsson commented earlier versions of the manuscript.

## REFERENCES

- Bjerring, H. C. 1989. Apertures of craniate olfactory organs. *Acta Zoologica* 70:71-85.
- Bryant, W. L. 1919. On the structure of *Eusthenopteron*. *Bulletin of the Buffalo Society of Natural Sciences* 13:1-59.
- Campbell, K. S. W. and R. E. Barwick 1984. The choana, maxillae, premaxillae and anterior palatal bones of early dipnoans. *Proceedings of the Linnean Society of New South Wales* 107:147-170.
- Chang, M.-M. 1991. "Rhipidistians", dipnoans and tetrapods. pp.3-28 in H.-P. Schultze and L. Trueb, (eds), *Origins of the higher groups of tetrapods, controversy and consensus*, Cornell University Press, New York.
- Clement, G. 2001. Evidence for lack of choanae in the Porolepiformes. *Journal of Vertebrate Paleontology* 21(4):795-802.
- Cloutier, R., and P. E. Ahlberg. 1996. Morphology, characters and interrelationships of basal sarcopterygians. pp. 445-479 in M. L. J. Stiassny, L. R. Parenti and G. D. Johnson (eds), *Interrelationships of Fishes*. Academic Press, New York.
- Cloutier, R., S. Loboziak, A.-M. Candilier and A. Blicek. 1997. Biostratigraphy of the Upper Devonian Escuminac Formation, Eastern Quebec, Canada: a comparative study based on miospores and fishes. *Review of Palaeobotany and Palynology* 93:191-215.

- Holmes, E. B. 1985. Are lungfishes the sister-group of tetrapods? *Biological Journal of the Linnean Society* 25:379-397.
- Holmgren, N. and E. A. Stensiö 1936. *Kranium und Visceralskelett der Akranier, Cyclostomen und Fische.* pp. 223-500 in L. Bolk, E. Göppert, E. Kallius and W. Lubosch (eds), *Handbuch der vergleichenden Anatomie der Wirbeltiere.* VI. Skelettsystem, Urban and Schwarzenberg, Berlin, Wien.
- Jarvik, E. 1937. On the species of *Eusthenopteron* found in Russia and the Baltic States. *Bulletin of the Geological Institution of the University of Uppsala* 27:63-127.
- Jarvik, E. 1942. On the structure of the snout of crossopterygians and lower gnathostomes in general. *Zoologiska Bidrag Uppsala* 21:235-675.
- Jarvik, E. 1972. Middle and Upper Devonian Porolepiformes from East Greenland with special reference to *Glyptolepis groenlandica* n. sp. and a discussion on the structure of the head in the Porolepiformes. *Meddelelser om Grønland* 187:1-295.
- Jarvik, E. 1980. *Basic structure and evolution of vertebrates.* Vol. 1. Academic Press, New York.
- Jarvik, E. 1981. Lungfishes, tetrapods, paleontology, and plesiomorphy. D. E. Rosen, P. L. Forey, B. G. Gardiner and C. Patterson 1981. *Systematic Zoology* 30:378-384.
- Johanson, Z. and P. E. Ahlberg 2001. Devonian rhizodontids and tristichopterids (Sarcopterygii; Tetrapodomorpha) from East Gondwana. *Transactions of the Royal Society of Edinburgh: Earth Sciences* 92:43-74.
- Jurgens, J. D. 1971. The morphology of the nasal region of Amphibia and its bearing on the phylogeny of the group. *Annale Universiteit Van Stellenbosch* 46:1-146.

- Long, J. A., R. E. Barwick and K. S. W. Campbell. 1997. Osteology and functional morphology of the osteolepiform fish *Gogonasus andrewsae* from the Upper Devonian Gogo formation, Western Australia. Records of the Western Australian Museum Supplements 53:1-89.
- Panchen, A. L. 1967. The nostril of choanate fishes and early tetrapods. Biological Review 42:374-420.
- Panchen, A. L. and T. R. Smithson 1987. Character diagnosis, fossils and the origins of tetrapods. Biological Review 62:341-438.
- Parent, N. and R. Cloutier. 1996. Distribution and preservation of fossils in the Escuminac Formation. pp. 54-78 in H.-P. Schultze and R. Cloutier (eds), Devonian Fishes and Plants of Miguasha, Quebec, Canada. Verlag Dr. Friedrich Pfeil, München.
- Rosen, D. E., P. L. Forey, B. G. Gardiner and C. Patterson 1981. Lungfishes, tetrapods, paleontology and plesiomorphy. Bulletin of the American Museum of Natural History 167:159-276.
- Schultze, H.-P. 1981. Hennig und der Ursprung der Tetrapoda. Paläontologie Zeitung 55:71-86.
- Schultze, H.-P. 1984. Juvenile specimens of *Eusthenopteron foordi* Whiteaves, 1881 (osteolepiform rhipidistian, Pisces) from the Late Devonian of Miguasha, Quebec, Canada. Journal of Vertebrate Paleontology 4:1-16.
- Schultze, H.-P. 1987. Dipnoans as sarcopterygians. Journal of Morphology Supplements 1:39-74.

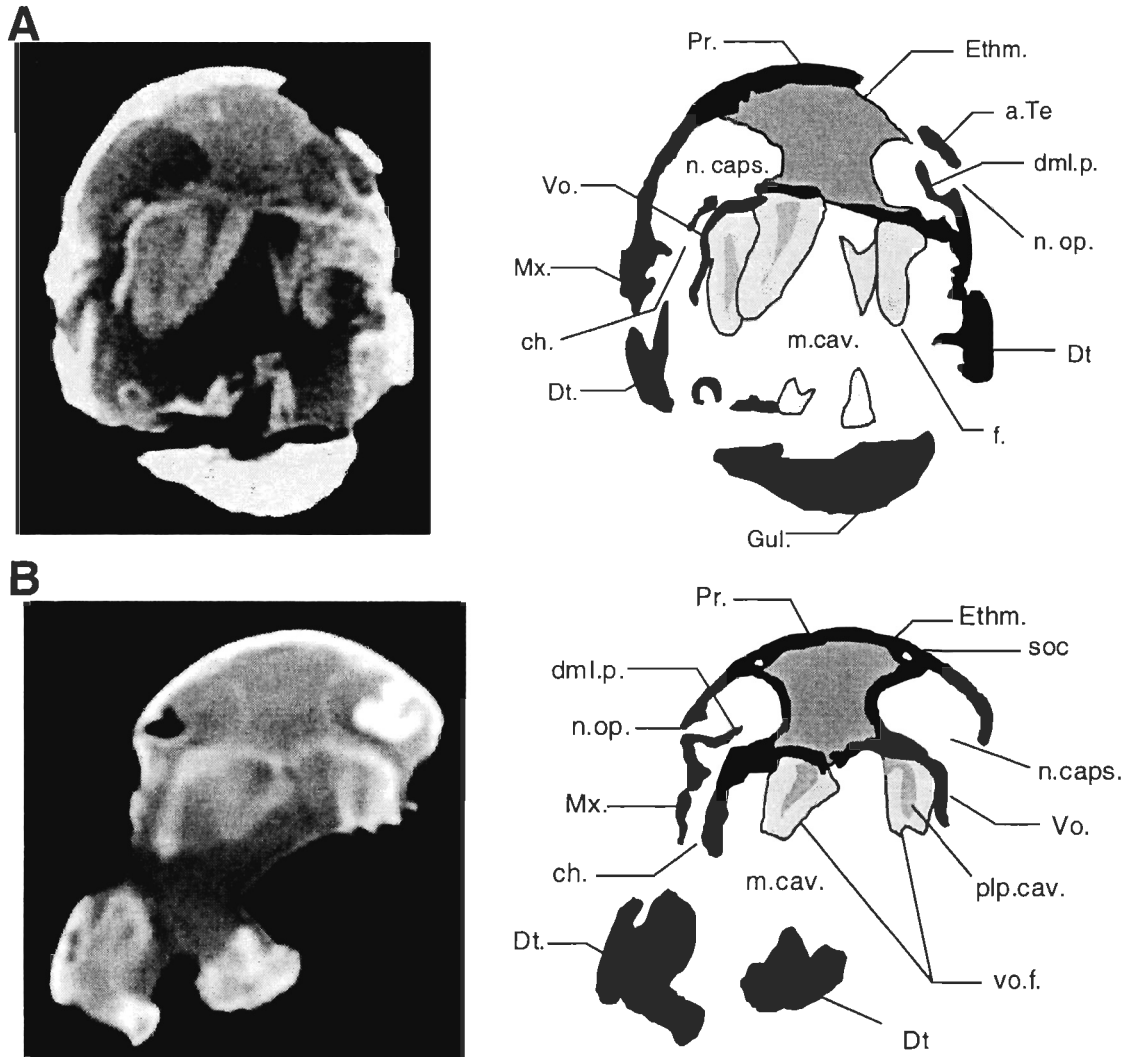
- Schultze, H.-P. 1991. A comparison of controversial hypothesis on the origin of tetrapods. pp. 29-67 in H.-P. Schultze and L. Trueb (eds), *Origins of the higher groups of tetrapods, controversy and consensus*, Cornell University Press, New York.
- Stensiö, E. 1921. *Triassic fishes from Spitzbergen. Part I.* A. Holzhausen, Vienna, 307p.
- Stensiö, E. 1922. Notes on certain crossopterygians. *Proceedings of the Zoological Society of London* 1922:1241-1271.
- Swofford, D. L. 2002. PAUP\*. *Phylogenetic analyses using parsimony (\*and Other Methods)*. Version 4. Sinauer Associates, Sunderland, Massachusetts.
- Vorobyeva, E. I. and H.-P. Schultze. 1991. Description and systematics of panderichtyid fishes with comments on their relationship to tetrapods. pp. 68-109 in H.-P. Schultze and L. Trueb (eds), *Origins of the Higher Groups of Tetrapods: Controversies and Consensus*, Cornell University Press, New York.
- Watson, D. M. S. 1926. The evolution and origin of the Amphibia. *Philosophical Transactions of the Royal Society of London (B)* 214:189-257.
- Zhu, M. and H.-P. Schultze. 1997. The oldest sarcopterygian fish. *Lethaia* 30:293-304.
- Zhu, M. and H.-P. Schultze. 2001. Interrelationships of basal osteichthyans. pp. 289-314 in P. E. Ahlberg (ed.), *Major events in early vertebrate evolution. Paleontology, phylogeny, genetics and development. Systematics Association Special Volume Series 61.* Taylor and Francis, London and New York.
- Zhu, M. and P. E. Ahlberg. 2004. The origin of the internal nostril of tetrapods. *Nature* 432:94-97.

**Table 1** Relative dimensions of nasal capsule related structures among three specimens of *Eusthenopteron foordi*. All measurements are given in percentage; naris height: proportion of snout height (lateral view); naris depth: proportion of snout width (scan view); nasal capsule width: proportion of snout width; passage depth: proportion of snout height; choana width: proportion of snout width.

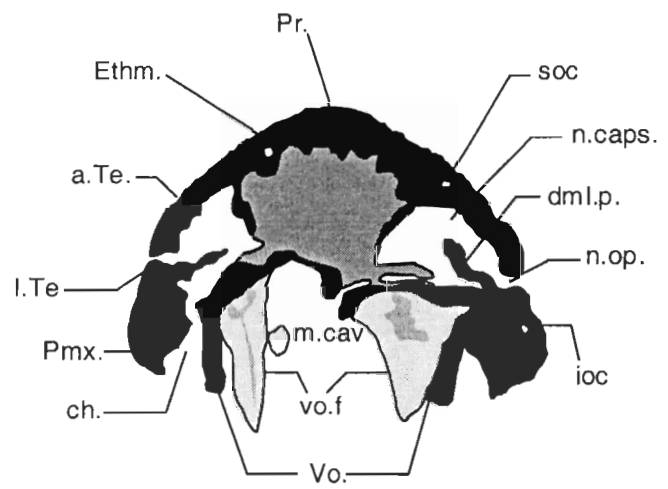
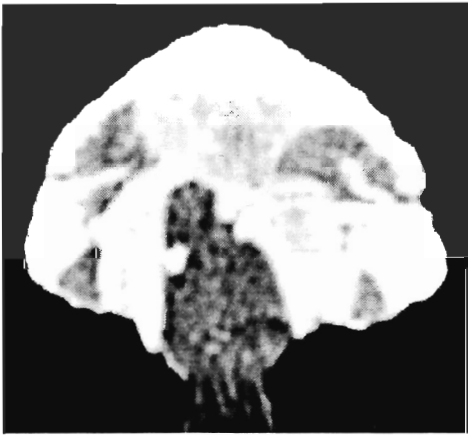
	Naris height	Naris depth	Nasal capsule width	Passage depth	Choana width
RM 14234	11,3	8,3	33,9	43,9	13,1
MHNM 06-1045	16,9	N/A	30,3	43,6	12,0
MHNM 06-1001A	7,6	5,2	35,9	45,0	13,9
Jarvik (1942; pl. 11)	12,2	4,9	33,0	37,7	12
Rosen <i>et al.</i> (1981)	N/A	N/A	N/A	N/A	5

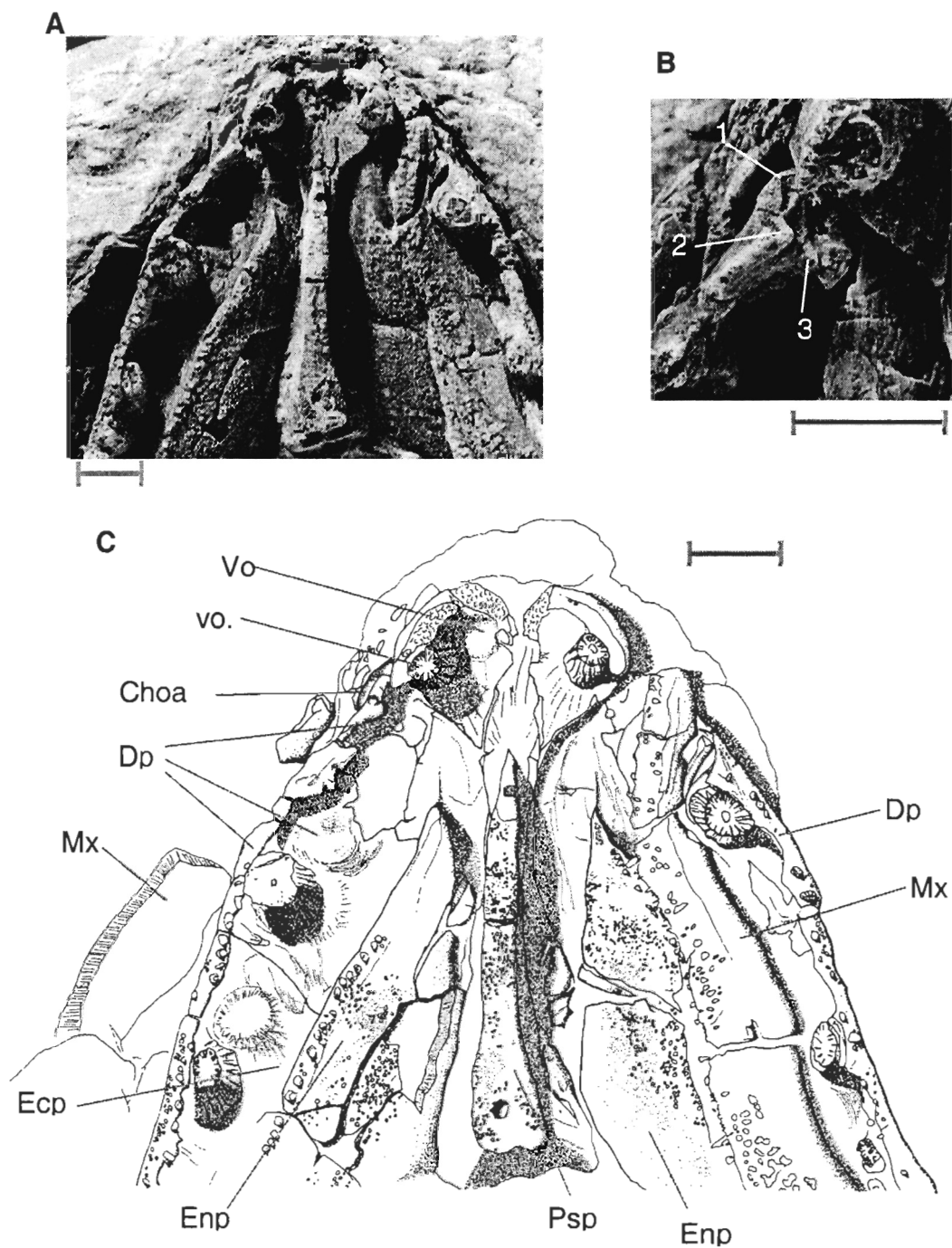
**Table 2** Results of phylogenetic analyses using PAUP\*4.0b10 on four previously published matrices.

	Trees	Steps	CI	RI
Cloutier & Ahlberg (1996) (PAUP version unknown)	54	277	0,578	0,818
Reanalysis unordered				
<i>Eusthenopteron foordi</i> with a choana	54	278		
<i>Eusthenopteron foordi</i> without a choana	18	278		
Character 48 deleted	54	276		
Zhu & Schultze (1997) (PAUP version unknown)	54	276	0,580	0,821
Reanalysis unordered				
<i>Eusthenopteron foordi</i> with a choana	54	276		
<i>Eusthenopteron foordi</i> without a choana	18	276		
Character 48 deleted	54	274		
Zhu & Schultze (2001) (PAUP 3.1.1)	45	464	N/A	N/A
Reanalysis unordered				
<i>Eusthenopteron foordi</i> with a choana	60	461		
<i>Eusthenopteron foordi</i> without a choana	60	462		
Character 113 deleted	60	459		
Johanson & Ahlberg (2001) (PAUP 4.0b2)	9	197	0,5685	0,7751
Reanalysis unordered				
<i>Eusthenopteron foordi</i> with a choana	6	193		
<i>Eusthenopteron foordi</i> without a choana	6	194		
Character 28 deleted	6	192		

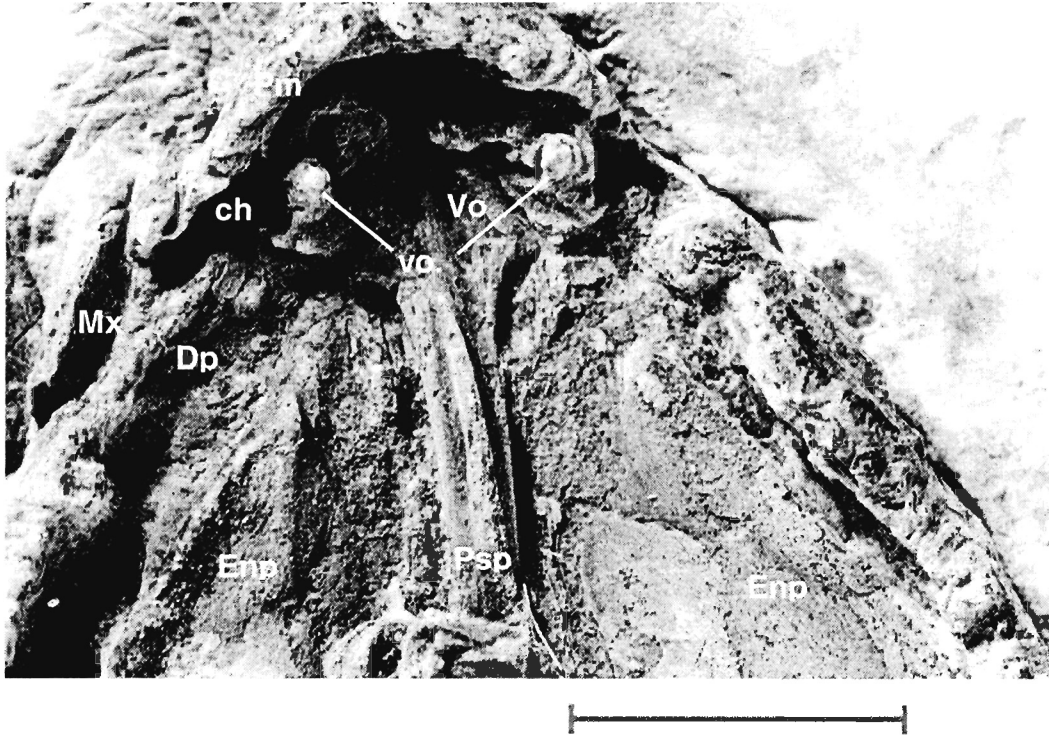


**Figure 1** Cross section in the nasal capsule region of *Eusthenopteron foordi*. **A.** Specimen MHNM 06-1001A (scan 8/36); **B.** Specimen MHNM 06-1045 (scan 8/16); **C.** Specimen RM 14234 (scan 102/110). Left column: Computed Tomography. Right column: Interpretation of the CT scan; black = bone, dark grey = ethmosphenoid, light grey = teeth. Abbreviations, **a.Te.:** anterior tectal, **ch.:** choana, **dml.p.:** dermintermedial process, **Dpl.:** dermopalatine, **Dt.:** dentary, **Ecpt.:** ectopterygoid, **Enpt.:** entopterygoid, **Ethm.:** ethmosphenoid, **f.:** fang, **Gul.:** gular plate, **ioc:** infraorbital canal, **l.Te:** lateral tectal, **m.cav.:** mouth cavity, **Mx.:** maxillary, **n.caps.:** nasal capsule, **n.op.:** nasal opening, **plp.cav.:** pulp cavity, **Pmx.:** premaxillary, **Pr.:** postrostral, **Psph.:** parasphenoid, **soc:** supraorbital canal, **Vo.:** vomer, **vo.f.:** vomerine fang.

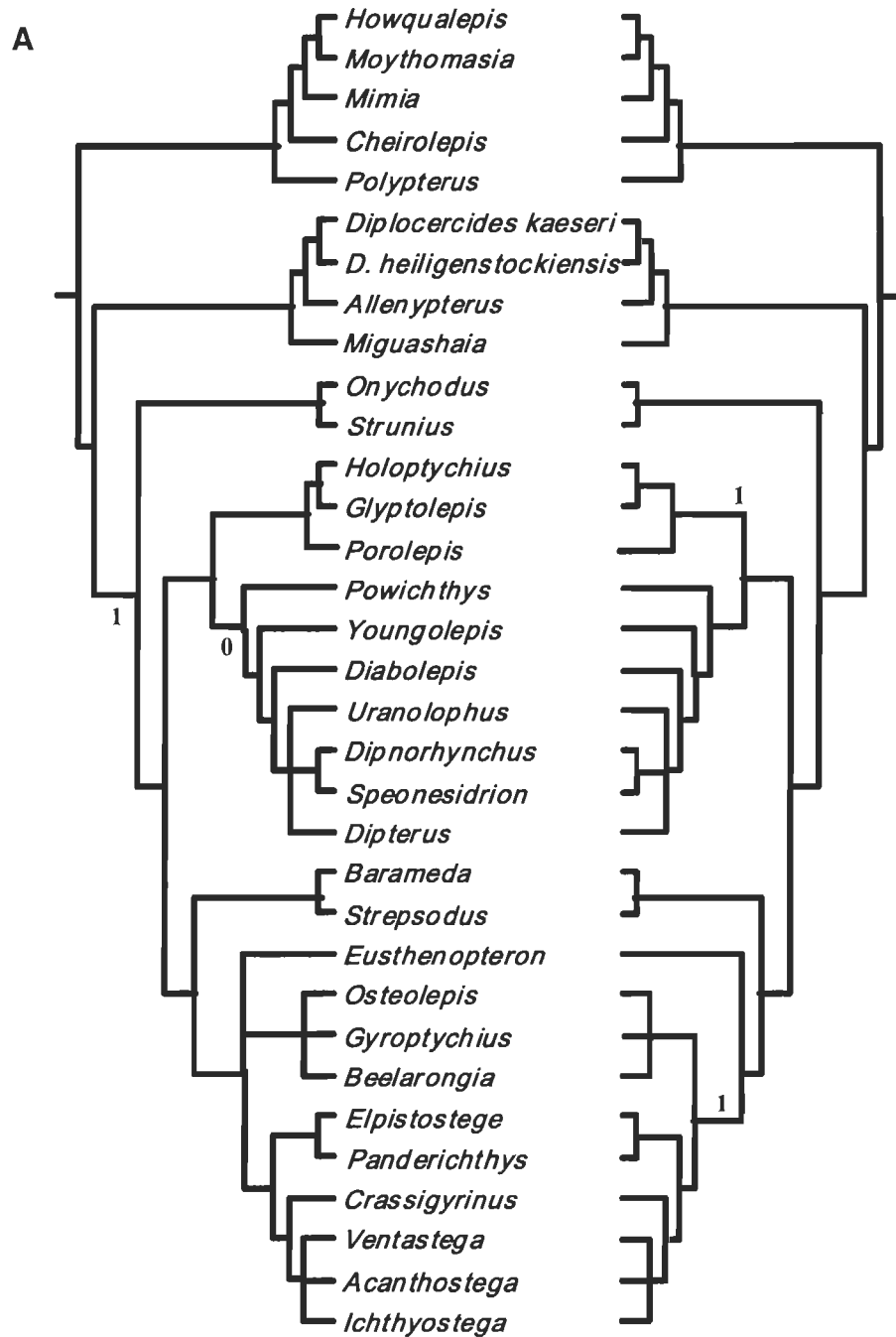
**C**



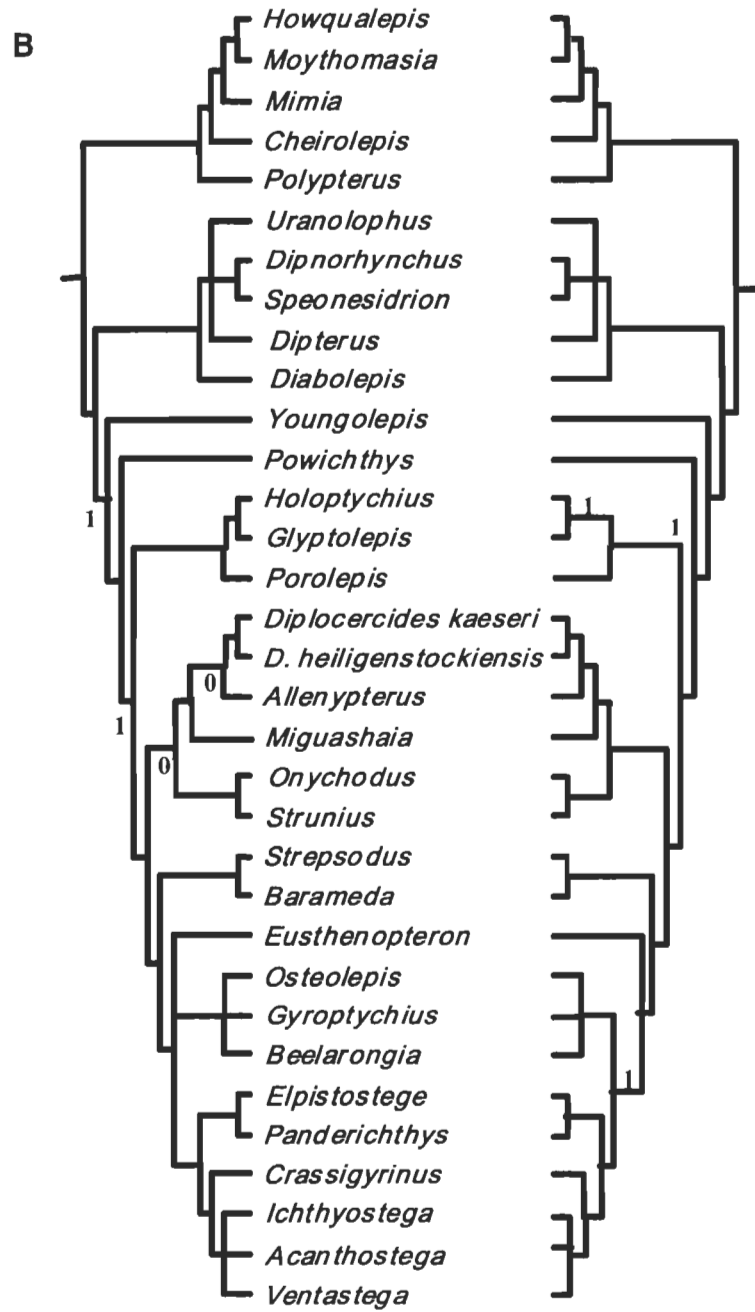
**Figure 2** *Eusthenopteron foordi*, specimen MHNM 06-719. A. Ventral view of the palate; B. Close-up of the choana area; C. Camera-lucida drawing of the specimen. Scale bars : 1 cm. 1, 2 and 3 identify facets on the head of the dermopalatine. **Dpl.:** dermopalatine, **Ecpt.:** ectopterygoid, **Enpt.:** entopterygoid, **Mx.:** maxillary, **Psph.:** parasphenoid, **Vo.:** vomer, **vo.f.:** vomerine fang.

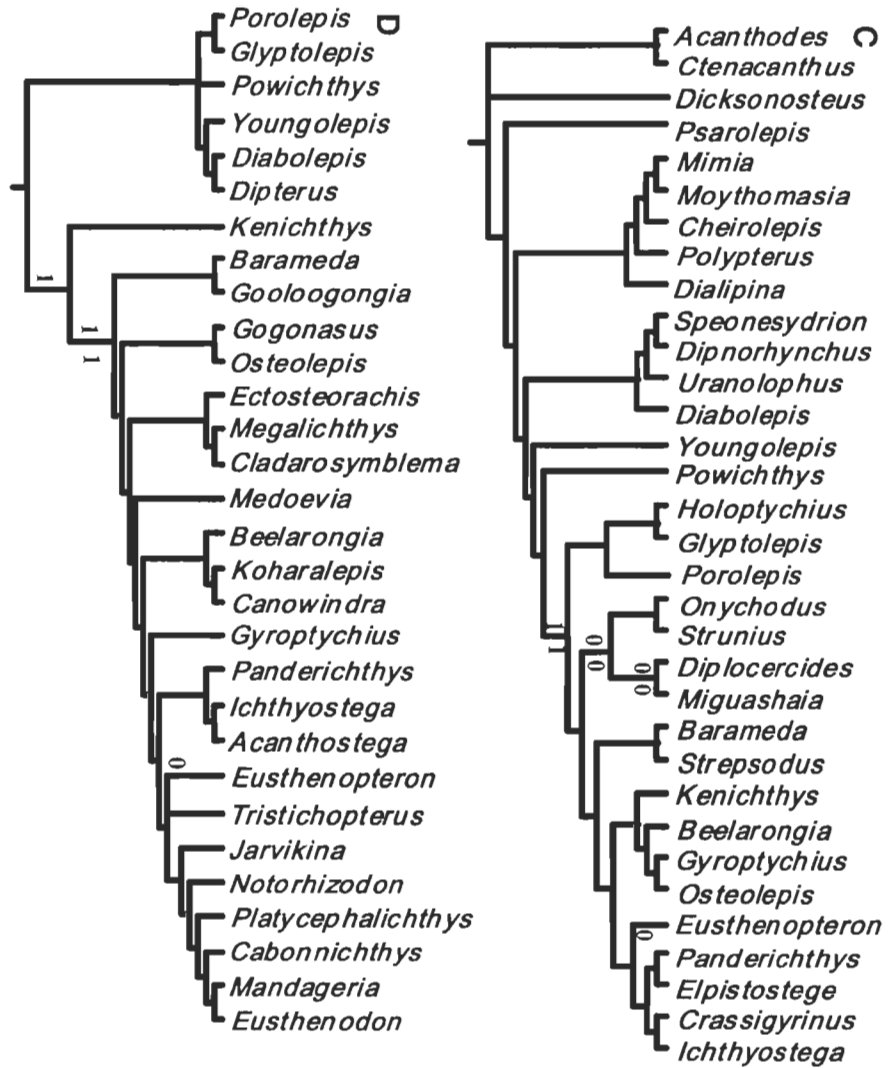


**Figure 3** *Eusthenopteron foordi*, specimen MHNM 06-220. Ventral view of the palate. Scale bar ; 1 cm. **ch.**: choana, **Dpl.**: dermopalatine, **Enpt.**: entopterygoid, **Mx.**: maxillary, **Pmx.**: premaxillary, **Psph.**: parasphenoid, **Vo.**: vomer, **vo.f.**: vomerine fang.



**Figure 4** Strict consensus trees obtained from previously published matrices. Trees obtained from: **A**. Cloutier & Ahlberg (1996); **B**. Zhu & Schultze (1997); **C**. Zhu & Schultze (2001); **D**. Johanson & Ahlberg (2001) matrices. 1 identifies appearance of the choana character, 0 identifies reversal of this character. Trees from original matrices are numbered on the right side of the branches, whereas trees from modified matrices (choana considered absent in *Eusthenopteron*) are numbered on their left side. **C** and **D** only have one tree because the topology remained the same after the matrix modification. Trees **B** and **D** show double appearance and/or reversal because it was not possible to know if the authors used “ACCTRAN” or “DELTRAN” options.





## CHAPITRE 2

# **Developmental Modularity and Saltatory Ontogeny in the Late Devonian Osteolepiform *Eusthenopteron foordi*.**

Joël Leblanc and Richard Cloutier

Laboratoire de Biologie évolutive, Université du Québec à Rimouski,

300 allée des Ursulines, Rimouski, Québec, G5L 3A1, Canada

[richard\\_cloutier@uqar.qc.ca](mailto:richard_cloutier@uqar.qc.ca)

RH : LEBLANC AND CLOUTIER - ONTOGENY OF *EUSTHENOPTERON*

## ABSTRACT

Sixty-five specimens of the Late Devonian osteolepiform *Eusthenopteron foordi* were studied in order to reconstruct its sequence of ossification. The specimens ranging from 27.0 to 270.6 mm in standard length represent a size series that was treated like a growth series thus revealing the growth pattern of the species. The presence and absence of all postcranial bony elements, with special emphasis on fin-systems, were recorded. The pectoral girdles (cleithra, clavicles and anocleithra) and the basal scutes at the base of unpaired fins are among the earliest postcranial structures to ossify. In the fins, the distal elements are the first to ossify, followed by proximal elements. The caudal part of vertebral column, as well as the distal bones of the second dorsal and anal fins, are the first endochondral bones to ossify. After a relative stagnation of the development, during which the other fins partly develop, the anterior part of the vertebral column suddenly settles in a short time. The general pattern of ossification shows a saltatory ontogeny: numerous bones appear in short time laps, and these events are separated by periods of slower development. A first threshold of accelerated development occurs at a standard length of ca. 42 mm (ossification of the posterior propulsive system), and a second one occurs at ca. 160 mm (ossification of the anterior part of vertebral column). Isometric growth for postcranial skeleton is confirmed in *E. foordi*. Study of the growth series also reveals a developmental modularity: the second dorsal and anal fins, appearing and growing in synchronicity, together form a module. This is comparable with the medial fins developmental modularity of all living actinopterygian and this is the first description of such a development for a fossil species.

## RÉSUMÉ

Soixante-cinq spécimens de l'ostéolépiforme *Eusthenopteron foordi* du Dévonien tardif ont été étudiés afin de reconstituer sa séquence d'ossification. L'échantillon, constitué de spécimens dont les longueurs standard allaient de 27,0 à 270,6 mm, représente une «série de taille» qui fut traitée comme une série de croissance révélant ainsi le patron de croissance de l'espèce. Les observations furent faites sur la base de la présence ou l'absence de tous les éléments osseux du squelette post-crânien, avec une attention particulière portée aux systèmes natatoires. Les ceintures pectorales (cleithra, clavicules, anocleithra) et les scutelles à la base de toutes les nageoires impaires sont parmi les premières structures postcrâniennes à s'ossifier. Dans les nageoires, les éléments distaux s'ossifient d'abord, suivi par les éléments proximaux. La partie postérieure de la colonne vertébrale, située dans la nageoire caudale, tout comme les os distaux de la seconde nageoire dorsale et de la nageoire anale, sont les premiers os endochondraux à s'ossifier. Après une stagnation relative du développement, pendant laquelle les autres nageoires se développent partiellement, la partie antérieure de la colonne vertébrale prend soudainement place en peu de temps. Finalement, la majeure partie du reste de la croissance est marquée par l'ajout constant et continu d'éléments, principalement dans la partie médiane de la colonne vertébrale. Le patron général d'ossification révèle une ontogénie saltatoire : plusieurs os apparaissent en peu de temps, et ces événements sont séparés par des périodes de développement plus lent. Une première poussée de développement accéléré se produit à une longueur standard d'environ 42 mm (ossification du système propulsif postérieur), et un autre a lieu à environ 160 mm (ossification de la partie antérieure de la colonne

vertébrale). Une croissance isométrique du squelette postcrânien est confirmée chez *E. foordi*. L'étude de cette série de croissance révèle aussi une modularité développementale: la deuxième nageoire dorsale et la nageoire anale, apparaissant et se développant en synchronisme, forme un module. Celui-ci est comparable à la modularité développementale retrouvée dans les nageoires médianes de tous les acitnoptérygiens vivants et il s'agit de la première description d'un tel développement chez une espèce fossile.

## INTRODUCTION

Skeletal ontogeny can be described in terms of morphometric changes (i.e., size and shape) as well as anatomical (e.g., ossification pattern) and histological changes. In either case, one has to observe growth series in living animals (e.g., Arratia et al., 2001; Grünbaum et al., 2003) or size series in extinct animals (Schultze, 1984; Carroll et al., 1999; Chipman and Tchernov, 2002; Cote et al., 2002). With respect to fossils, as many different sized specimens as possible of the same species are needed, allowing to compare the anatomy of the smallest individuals up to those of the largest individuals. Furthermore, the estimate of intraspecific variation would be more accurate if based on larger sample size. Size series of extinct species are rare and younger individuals are especially uncommon. A size series is not exactly equivalent to a growth series; it is actually a static sample of a species or a population (Schultze, 1984). But, as explained by Schultze (1984), it is reliably representative of a growth series. Such inferences of growth series from size series have been carried out for a few fossil fishes: the placoderm *Bothriolepis canadensis* (Werdelin and Long, 1986) and *B. nitida* (Weems, 2004), the actinopterygian *Elonichthys* (Schultze and Bardack, 1987), the dipnoan *Scaumenacia curta* (Cloutier, 1997), and the osteolepiform *Eusthenopteron foordi* (Thomson and Hahn, 1968; Schultze, 1984).

*Eusthenopteron foordi* Whiteaves 1881, from the Upper Devonian Escuminac Formation of Miguasha, Québec, Canada, is one of these rare fossil species to be a candidate for such an ontogenetic study. Phylogenetically, *Eusthenopteron* is informative because it belongs to the Tetrapodomorpha, the clade inclusive of elpistostegalians and tetrapods (Cloutier and Ahlberg, 1996; Zhu and Schultze, 2001). For the past 120 years,

more than 2200 specimens (Parent and Cloutier, 1996) of *E. foordi* have been found in the Escuminac Formation. Although *E. foordi* is the most abundant osteolepiform, most of our knowledge on this species is typological with only a few exceptions [see Cloutier (1996) for a review]. Nevertheless, the sample size is large enough and varied enough to allow description of its ontogeny, either in terms of morphometry (Thomson and Hahn, 1968; Schultze, 1984), anatomy (Andrews and Westoll, 1970), and sequence of ossification (Cote et al., 2002). Many specimens show a good state of preservation allowing observation of fine details of the endoskeletal elements. *Eusthenopteron* specimens range in size from small “juveniles” approximately 3 cm long to large “adults” of more than 1 m (Parent and Cloutier, 1996). Frequently, it is mentioned that *E. foordi* reached more than 1.5 m in length (Andrews and Westoll, 1970; Schultze 1984; Cote et al. 2002). However, the largest complete specimens (e.g., CMNH 8158, SMNH P.222) are approximately 1m long. Partial specimens suggest that they could reach larger size. Based on lower jaw and skull proportions (Schultze, 1984), standard length of the largest known specimens (MHNM 06-496, 06-1001A) is estimated to 118 cm.

The first mention of ontogenetic changes in *Eusthenopteron foordi* was done by Stensiö (1925). In his description of the caudal fin, he interpreted the change in size and shape of the median lobe as a growth stage. Based on 29 specimens, Thomson and Hahn (1968) concluded that the growth of *E. foordi* was differential; the cranial proportions and the relative position and the shape of fins were considered to vary during growth. Thomson and Hahn (1968) clearly documented the caudal change reported by Stensiö (1925). Andrews and Westoll (1970) described in great details the postcranial morphology of *E.*

*foordi* based on more than 25 specimens. However, the only ontogenetic comments concern the shape of the cleithrum, the area of attachment of the scapulocoracoid, and the median fin supports (Andrews and Westoll, 1970: Text-fig. 3 and 28, respectively). Using additional specimens from the Musée d'Histoire Naturelle de Miguasha, Schultze (1984) corroborated allometric changes in the skull development of *E. foordi* using Cartesian transformations; most of the changes are imputable to the relative decrease of the orbit diameter. However, in contrast to Thomson and Hahn (1968), Schultze (1984) proposed that the position of fins did not display an allometric pattern. Recently, Cote et al. (2002) studied the growth of *Eusthenopteron* in terms of the sequence of ossification of postcranial bones, primarily those forming the vertebral column. They concluded, based on 27 specimens smaller than 30 cm, that the vertebral development displayed a complex pattern of ossification. Especially, the bidirectional development of the vertebral column made the growth of *E. foordi* unique among osteichthyans.

The absence of postcranial allometry (Schultze, 1984) and the relatively constant increasing pattern of ossification (Cote et al., 2002) could lead one to consider the growth pattern of *E. foordi* to be gradual. Gradual ontogeny has been traditionally considered to be the generalized growth pattern; however, a few studies on recent fishes have shown saltatory events during larval growth (Balon, 1979, 1986, 1999). According to Balon (1986, 1999), the early development of fishes is characterized by the occurrence of rapid integrated morphological changes or saltatory ontogenetic events. The main objectives of our study are: (1) to describe the ossification sequence of all the postcranial elements of *Eusthenopteron foordi*, with a special emphasis on fin development; (2) to correlate

changes in the sequence of ossification with morphometric changes; and (3) to describe *E. foordi* ontogenetic pathway in terms of gradual and saltatory events.

## **MATERIAL AND METHODS**

### ***Specimens***

All the specimens of *Eusthenopteron* come from the Escuminac Formation, which has a thickness of ca. 119 m (Cloutier et al., 1997). Cloutier (1997) suggested that the sediments were deposited over a period of one to two million years. For the present article, we consider this time lap to be minor in term of evolutionary changes for this species. Thus, we consider all specimens of *E. foordi* to belong to a single species.

Sixty-five specimens from five different collections were studied (Fig. 2): American Museum of Natural History, New York City, New York, U.S.A. (**AMNH**); Field Museum of Natural History, Chicago, Illinois, U.S.A. (**FMNH**); Musée d'Histoire Naturelle de Miguasha, Miguasha, Québec, Canada (**MHNM**); Canadian Museum of Nature, Ottawa, Ontario, Canada (**CMN**); and Collection René-Bureau from Université Laval, Québec City, Québec, Canada (**UL**).

### ***Sequence of ossification***

An ossification sequence corresponds to the successive ossification of bones during the early development of a vertebrate. The sequence of ossification of all the elements associated with the appendicular and axial skeleton (ca. 480 possible elements for *E. foordi*) was described in terms of three major components: (1) the absolute timing (in terms

of standard length of the specimens) which provides the temporal sequence of appearance of the bones; (2) the temporal information is converted in relative timing, or the order of formation of these structures; and (3) when dealing with serial or iterated elements and morphological systems, direction of ossification is inferred. With respect to living fishes, the sequence is usually done by sampling individuals at a known moment of their development. The temporal component can either be given in terms of (1) days post-hatching, (2) accumulated degree days post-activation (Pinder and Gozlan, 2004), or (3) hours post-activation (Pinder and Gozlan, 2004). For each specimen, measurements are taken and visible bony and cartilaginous structures are noted. A *growth series* is thus obtained. With fossil organisms, the actual age of each animal is difficult or impossible to assess and only a *size series* can be established. In such case, time is replaced by a metric dimension of the specimens, assuming that larger animals are older, as did Schultze (1984). Even with living organisms, sequence can be constructed using the size as a temporal estimate of growth (Mabee et al., 2000; Mabee and Trendler, 1996). Specimens are sorted by length and it is then possible to note how many new bony elements are present in each of them that were not visible in the previous specimens. The resulting sequence of ossification is an atlas of the skeleton of the animal at different periods of its development. With respect to fossils, a few constraints make this exercise difficult and can introduce variation in the sequence: (1) the incompleteness of the specimens; (2) the position in which the fossil is preserved, revealing only certain structures and making the measurements difficult to take; (3) scales can cover internal structures; (4) the state of preservation can vary among specimens; and (5) the incompleteness of the fossils forces

one to estimate the size of the specimen which is the main sequential criteria. The complete sequence of ossification for the appendicular and axial skeleton is given in figures 2 and 7.

### ***Measurements***

The 20 measurements proposed by Schultze (1984, Fig. 1) were taken on each specimen. Measurements were taken using a dial caliper with a precision of 0.1 mm. Statistics were performed with MS Excel version 97.

### ***Bone terminology***

The terminology of the vertebral column elements of *Eusthenopteron foordi* follows that of Andrews and Westoll (1970). Numbers from 1 to 60 were assigned to each vertebral unit, starting with the anteriormost vertebra. The trunk vertebral units comprise two intercentra, two pleurocentra, a neural arch/spine complex. Vertebral units from 32 to 60 comprise a haemal arch/spine complex. Caudal units (from 42 to 60) also include a ventral caudal radial. In order to establish the position of a specific vertebra, especially when the vertebral column was incompletely preserved, benchmarks based on Andrews and Westoll's (1970) reconstruction were used: the vertebra 27 is at the level of the first dorsal fin; vertebra 39 is at the level of the second dorsal fin; vertebra 41 is at the level of the anal fin; vertebra 32 is the first one to have a haemal spine; and vertebra 42 is the first one to be associated with a ventral caudal radial. In order to use such a method of vertebrae

identification, we must assume that intraspecific variation in terms of the number of vertebrae in *E. foordi* is minor (see Andrews and Westoll, 1970).

## RESULTS

In our sample of 65 specimens, the smallest individual was 27.0 mm long (MHNM 06-234) in standard length, whereas the largest was 270.6 mm long (AMNH 7535). The average difference of standard length between two consecutive specimens is 3.8 mm. Only 32 specimens out of 65 were complete. Standard length (S.L.) was estimated either from the distance between the insertion points of the two dorsal fins (D1-D2) or between the insertion points of the second dorsal and the caudal fin (D2-C) in order to sort all specimens (incomplete and complete) into a size series. Regression lines were obtained from complete specimens and from measures given by Thomson and Hahn (1968, 14 specimens from Table I) and Schultze (1984, 30 specimens from Table 3). We used our own measurements in the case of specimens already measured in previous studies. The regression equations (Fig. 1) are the following: (1)  $S.L. = 6.6078 (D2-C) + 22.132$ ; and (2)  $S.L. = 6.029 (D1-D2) + 4.1136$ . The  $R^2$  values are high for both regressions (over 0.95); thus, suggesting that both equations provide reliable estimates of standard length. When D1-D2 and D2-C values were available on an incomplete specimen, the standard length was calculated by taking the mean value of the two estimated lengths. When only a little part of the specimen was missing, only the most logical result of both equations was considered. Estimated standard lengths and measured standard length are given in figure 2. The mean standard length of the sample is 143.4 mm (S.D. = 74.0).

In order to describe morphometric changes, the distances between the posterior margin of the operculum and different fin insertion points [first dorsal (Fig. 3A), second dorsal (Fig. 3B), pelvic (Fig. 3C), anal (Fig. 3D), upper caudal (Fig. 3E) and lower caudal (Fig. 3F)] are plotted against the standard length of specimens for which these measurements were available. The  $R^2$  of each regression line are all greater than 0.94. A slight tendency to allometric growth seems visible for the six relationships; points are mainly above the regression line at both extremities, whereas they are below the line in the central part. In order to verify whether those relationships are isometric or allometric, data were  $\log_{10}$  transformed and 95% confidence interval for the slope of the major axis were calculated (Table 1; Jolicoeur, 1968; Cloutier, 1997). None of the major axis slope differs significantly from the isometric value of 1. This reveals that the proportions of *E. foordi* (i.e., the relative positions of the different fins along the body axis) were not changing during growth as suggested by Schultze (1984).

Dermal and endochondral bones are well preserved in most specimens of *E. foordi*. As reported by Andrews and Westoll (1970), internal skeleton is often composed of very lightly ossified cancellous bones. Frequently, the cancellous nature of the endochondral bone is revealed by calcitic infilling. Furthermore, these tissues are associated with a light brown color of the bones, in contrast to the frequent dark brown color of dermal bones.

### ***Skull***

Even in the smallest specimens, external dermal bones of the head were ossified. For the 47 specimens having the head preserved, 10.7% were compressed dorsoventrally

and 89.3% were compressed laterally. The relative degree of crushing (assumed to be related to the degree of ossification) seems to be the same for the 47 specimens; thus the solidity of the neurocranium does not seem to be related to the length of the studied specimens. However, large specimens of *E. foordi* have sufficiently ossified neurocranium to be preserved in three dimensions with only slight deformation owing to taphonomical processes (e.g., MHNM 06-1045, MHNM 06-1001A, RM 14234; Leblanc and Cloutier, in prep.). Although most, if not all, external dermal bones are ossified in the smaller individuals, first indicator of neurocranial ossification seems to be absent in specimens smaller than 30 cm.

Rare are the specimens in which hyoid and branchial elements are preserved. Among the 65 examined specimens, specimen UL 265 (S.L.: 53.7 mm) is the smallest one to display some ossified branchial elements (Fig. 4). Two rod-like elements located at the level of the pectoral girdle could represent ceratobranchials. These fine bones are preserved mainly as a calcite infilling of the original structures.

### ***Sequences of ossification of the fins***

Sequence of ossification is discussed by morphological systems – the fins. The description of each fin integrates the absolute timing, relative timing and direction of ossification. Figure 5 synthesizes the sequences of ossification of all fins of *Eusthenopteron foordi*.

**Pectoral fins** - In the smallest specimen (MHNM 06-234; S.L.: 27.0 mm), only the postcleithra are visible. The cleithra appear in the second smallest specimen (MHNM 06-235; S.L.: ca. 33 mm). Specimen MHNM 06-235 being compressed dorsoventrally, it is not possible to see if the clavicles were present. Anocleithra and clavicles are present in a specimen as small as 53.7 mm (UL 265, Fig. 4). The basal scutes are also visible in the pectoral fin of specimen UL 265 (Fig. 4). Two radials are present at a standard length of 66.0 mm (MHNM 06-213). The next structures to be seen simultaneously are the ulna and radius, at a length of ca. 119 mm (CMN 52263). And finally, the humerus ossifies at a length of ca. 159 mm (CMN 52264). The pectoral fins of *E. foordi* are thus ossifying in a distal to proximal direction.

**Pelvic fins** - In the pelvic fins, the basal scutes appear at a length of 44.5 mm (MHNM 06-535). Two radials are first visible at a length of ca. 111 mm (MHNM 06-59). The tibia is first seen in a ca. 119 mm long specimen (CMN 52263), the fibula in a specimen ca. 159 mm long (CMN 52264), whereas the pelvic girdle occurs only at 177.1 mm (CMN 4415). The femur is visible relatively late in ontogeny, in a 179-mm-long specimen (AMNH 5903). Like the pectoral fin, not taking the girdle into account of, the pelvic fin undergoes a distal to proximal development.

**First dorsal fin** - The first dorsal fin contains only two endochondral bones: a basal plate and a radial. Although the basal scutes appear early (41.8 mm, AMHN 7687), the first endoskeletal element to be visible is the radial, at a length of 59.6 mm (MHNM 06-238).

The first specimen to reveal an ossified basal plate is AMNH 5906 at a standard length of 81.1 mm. The direction of ossification of this fin is thus from distal to proximal. As illustrated by Andrews and Westoll (1970), the proximal end of the basal plate expands during growth.

**Second dorsal fin** - With the exception of the basal scutes that are present in AMNH 7687 (41.8 mm), distal radials ossify first, then followed by the basal plate. At a standard length of 44.5 mm, specimen MHNM 06-535 shows the second and the third radials in the second dorsal fin; the first radial is visible at 54.2 mm (UL 121). The basal plate finally appears at a length of ca. 111 mm (MHNM 06-59). At this stage, the basal plate is a narrow, rod-shaped element (Fig. 6), but subsequently, the distal part of the plate expands anteriorly in larger specimens. The pattern of development of the second dorsal fin is from distal to proximal.

**Anal fin** - The anal fin has a developmental pattern similar to that of the second dorsal fin. The three radials are seen at a length of 44.5 mm (MHNM 06-535) and the scutes are visible in a specimen of 53.7 mm (UL 265). The basal plate ossifies later, at a length of ca. 111 mm (MHNM 06-59). As for the second dorsal fin, the basal plate is initially rod-like and narrow (Fig. 6), becoming larger in its distal part in larger specimens. In contrast to Cote et al.'s (2002) interpretation of specimen MHNM 06-238, a single radial is present rather than two.

**Vertebral column and caudal fin** - The complete sequence of ossification for the axial skeleton including the caudal fin is presented in figure 7. Ossification primarily occurs in posterior elements, in the region of vertebral units 45 to 52, i.e. in the caudal fin. Neural spines 46 and 47 in the caudal fin are visible in a specimen of 36.4 mm (MHNM 06-13) and ventral caudal radials 45 to 53 are ossified in a specimen of 44.5 mm (MHNM 06-535). Specimen MHNM 06-535 is the first one in which nine ventral radials are present in the caudal fin. Neural spines 45 to 49 are also visible. These observations of specimen MHNM 06-535 differ from that of Cote et al. (2002); they had reported three neural arches with spines (instead of five), four ventral caudal radials (instead of nine), and no radials in the anal fin (instead of three).

Haemal spine 45, in the caudal fin, is the first to appear, being observable in a 53.7 mm long specimen (UL 265).

Our observation of specimen MHNM 06-238 (S.L.: 59.6 mm) also slightly differs from the description of Cote et al. (2002). They mentioned that the specific number of neural spines and ventral radials in the caudal fin are difficult to establish, and illustrated five of each in their drawing (Cote et al. 2002, Fig. 3C). We counted eight neural spines and eight ventral caudal radials.

From the vertebrae 46-47 area, neural spines successively ossify backward to reach their maximum posterior position at a standard length of 59.6 mm (MHNM 06-238); from 61.8 mm (FMNH UF 379), they ossify forward up to vertebra 42. The next anterior occurrence of neural spine will only happen at a length of ca. 159 mm (vertebra 1; CMN 52264). Our interpretation of specimen MHNM 06-30 (ca. 105 mm) also differs from that

of Cote et al. (2002). They mentioned the presence of six neural arches with spines, four caudal radials, three radials in the anal fin and both, the basal plate and the radial in the first dorsal fin. We noted the presence of eight neural arches with spines, eight ventral caudal radials, two radials in the anal fin and the absence of bone in the first dorsal fin. Cote et al. (2002) only reported the basal plate of the anal fin for specimen MHNM 06-59 (S.L.: ca. 111 mm), whereas we also saw the three radials of this fin (Fig. 6); they illustrated (Fig. 3E) six neural spines, five haemal spines and seven ventral caudal radials, whereas an additional element is present for each structure (Fig. 6).

At a standard length of ca. 62 mm, the caudal ventral radials are ossified from their maximum anterior position (vertebra 42) to vertebra 53. They only begin posteriorly ossification at a standard length of ca. 148 mm (AMNH FF 10187). This ossification is thus bidirectional from the vertebrae 45-53 region. In the early stages, the state of preservation of the ventral caudal radials provides information on the degree of ossification (Fig. 8). In small specimens [e.g., UL 95 (S.L.: 59.9 mm) and FMNH UF 379 (S.L.: 61.8 mm)], some of the radials seem to be collapsed longitudinally in the central axis of the bone, thus forming a longitudinal groove along the bone. In young individuals, radials were only weakly ossified; the main core of the radials was composed of poorly developed cancellous bone whereas peripheral bone was thin. During early taphonomic process, the weak peripheral bone crushed in the middle of the radials, thus forming a longitudinal groove. Among the larger individuals, this feature is only seen in three specimens [AMNH 5957 (S.L.: ca. 219.0 mm), AMNH 8904 (S.L.: 242.2 mm), AMNH 7535 (S.L.: 270.6 mm)]. However, in each of these specimens, only one or two radials associated with

vertebrae 46-48 have this feature. The degree of ossification provides support in favor of a weak bone density in the early stages of development.

Haemal spines, even if the first one (no. 45) is present in a small specimen (UL 265, S.L.: 53.7 mm), begin to ossify later than neural spines and ventral radials. The following haemal spines take place at a standard length of 102.3 mm (FMNH UC 2127) and they progress bidirectionally from the area of vertebrae 42-46. Haemal spines occur gradually until they reach their foremost position (vertebra 32) at a standard length of ca. 198 mm (MHNM 06-367), and their hindmost position (vertebra 57) at ca. 254 mm (FMNH 121-61).

The anterior part of the vertebral column only begins ossification at a relatively large standard length. Intercentra of vertebrae 1, 20, 21 and 22 are present in NMC 52264 (S.L.: ca. 159 mm). This specimen also displays a neural spine at the level of the first vertebra. At a length of 163.8 mm (MHNM 06-1544), intercentra 1 to 37 and neural arches and spines 1 to 28 are visible. This important modification is quickly followed by the appearance, at ca. 174 mm, of pleurocentra 4 to 10. However, the following pleurocentra appear much later, as revealed by 242.2-mm-long specimen AMNH 8904.

### ***Disparity and reliability of the sequence***

While establishing growth (or size) series, one has to deal with the intraspecific variability of the studied species. In order to detect the events that appear unusually early in a few individuals, Maisano (2002) introduced the concept of 'disparity' to designate the departures from the expected occurrence of skeletal events within a growth series. A

disparity estimate can be calculated for a growth series by dividing the total number of nonoccurrences of events after their initial appearance by the total number of occurrences of all events (Maisano, 2002). The ossification sequence for the fin elements of *Eusthenopteron foordi* is presented in Figure 2, each dark rectangle indicating the presence of a structure in a specific length specimen. The total number of non occurrences of elements after their initial appearance is 584 and the total number of occurrences of all elements is 515, for disparity estimate of 113% (not taking account of the missing parts of specimens, in light grey in Fig. 2). This high result can be explained in part by the inevitable incompleteness of fossils due to taphonomic processes. The absence of an element in a specimen does not mean the specimen did not have it at the moment of its death. For example, the basal scutes are fragile structures known to be not preserved in most of large specimens of *E. foordi*. Neglecting it from the calculation gives a lower disparity estimate of 80%. Despite, we can assume that this estimate would surely be lower if this study had been done with living material, as was its purpose when created by Maisano (2002), it is impossible to really know how much of this percentage is due to real precocity in occurrence of some elements and how much is due to fossil incompleteness. A further investigation for each element can be relevant.

In order to evaluate inter-individual variability in the sequence for each element, we investigated the degree of completeness of the sequence of ossification presented in figure 2. For each structure of the appendicular skeleton (excluding caudal fin), three counts are conducted (Table 2): (1) the actual number of specimens in which a structure has been observed; (2) the expected number of specimens in which the same structure should be

present; the maximal gap in the sequence in terms of (3) the number of specimens lacking the structure, and (4) the difference in standard length. Only the specimens for which the parts are preserved are taken into account in these four counts. The expected number of specimens corresponds to the number of specimens longer (in terms of standard length) than the smallest specimen that displays a structure. The reliability of a structure could either be influenced by (1) developmental plasticity, (2) intraspecific variability, or (3) artefactual absence of the structure owing to taphonomic bias.

In order to evaluate the reliability of a structure, a reliability index (RI) is calculated for each of them by dividing the actual number of specimens having a structure ossified by the number of specimens expected to have this structure. A high RI (over 0.50) means that many specimens expected to have a structure do have it and that the variability for this structure is low. All structures of the second dorsal and anal fins (with the exception of the basal scutes) are reliable and poorly variable.

When the RI is low (under 0.50), the sample might be less reliable for this structure, especially when there is an important gap in the early part of the ontogenetic sequence. It could suggest that the first specimen to present an ossification of this structure was likely abnormal with respect to the average (or typical) development of the species. For example, the radial of the first dorsal fin has a RI of 0.38; it is first visible in MHNM 06-238 (S.L.: 59.6 mm), but the radial is not seen in the next 16 specimens; it is visible again at a standard length of ca. 129 mm (MHNM 06-1301). It is thus likely that specimen MHNM 06-238 has undergone ossification of this element earlier than the standard pattern for *E. foordi*.

The mean RIs for each of the fins are: 0.31 for the pectoral, 0.30 for the pelvic, 0.39 for the first dorsal, 0.62 for the second dorsal, and 0.66 for the anal. The mean RI for the complete fin ontogenetic pathway of *E. foordi* is equal to 0.45. The size series thus seems reliable only for the second dorsal and anal fin, but, again, it becomes more reliable if we remove the basal scutes from the data; respectively 0.35, 0.34, 0.44, 0.73 and 0.76. For the complete ontogenetic pathway, it rises to 0.51. Noticeable is the similarity of the RI amongst different fins. The paired fins have almost the same RI, and the second dorsal and the anal fins are also close.

The disparity estimate (113%, or 80% without basal scutes) and the mean values of the RIs (0.45, or 0.51 without basal scutes) are compatible, both revealing a weak reliability for the sample.

The mean gap is equal to 2.89 (SD = 2.87, n = 201 gaps). The mean maximal gap for the 25 fin structures is 7.12. The relative position of the maximum gap can be used to interpret potential causes. The greater the gap is, the least likely it is that each specimen expected to have a structure lacks it owing to taphonomic bias. If the gap is situated later on during ontogeny (e.g., the radials of the pelvic fins), it is more likely that it is the result of taphonomic bias or sampling artefact.

### ***Relative order of ossification of the fins***

The first appendicular elements to form (excluding the lepidotrichia) are the dermal bones composing the pectoral girdle. It is seen in the smallest known specimen which is only 27.0 mm in standard length (MHNM 06-234). In this specimen, the postcleithra are

clearly visible but the presence of cleithra is unclear. However, cleithra appear in the next specimen (MHNM 06-235, S.L.: ca. 33 mm).

The relative order of ossification for *E. foordi* fins is as follows: (1) caudal, (2) second dorsal and anal, (3) first dorsal, (4) pectoral and (5) pelvic fins. The first endoskeletal fin supports to ossify belong to the caudal fin; neural spines 46 and 47 are visible in a specimen of 36.4 mm (MHNM 06-13). Shortly after, at a length of 44.5 mm (MHNM 06-535), radials appear simultaneously in the second dorsal and in the anal fins. Radials 2 and 3 are formed in the second dorsal fin, whereas the three radials are already present in the anal fin. At a length of 54.2 mm (UL 121 A/B), radials of the anal and second dorsal fins are all present. Up to a length of 81.1 mm, the length at which the basal plate of the dorsal fin is visible, there is no major fin modification.

Basal plates of dorsal and anal fins are all visible at a standard length of ca. 111 mm (MHNM 06-59). Ulna and radius in the pectoral fin are visible at a length of ca. 119 mm (CMN 52263). At ca. 159 mm (CMN 52264), all the fin elements of the fish are set up except the proximal bones of the pelvic fins. The femur finally appears at a length of ca. 179 mm (AMNH 5903 A/B).

### ***Basal scutes***

The basal scutes at the base of unpaired fins are the first dermal elements to form after the pectoral girdle (Fig. 9). Those scutes ossify before any endochondral element of the appendicular system with the exception of the anal fin. Their first occurrences are for both dorsal fins at 41.8 mm (AMNH 7687, Fig. 9A) and associated with the anal fin at 53.7

mm (UL 265). In paired fins, the scutes are visible at 53.7 mm for the pectoral fins (UL 265) and at 44.5 mm for the pelvic fins (MHNM 06-535).

Basal scute growth center is visible owing to the presence of radiating ridges from the focus of the bone (see Fig. 9D). Growth center seems to be located in the most anterior part of the scute suggesting an allometric backward growth. Basal scutes are well developed and especially large relatively to body size in small individuals. In UL 121A (S.L.: 54.2 mm; Figs. 9C, 9D), the basal scutes at the base of the anal fin reach 5.0 mm (9.2% of the standard length). In a larger specimen (MHNM 06-159, ca. 184 mm), this proportion falls to 5.6% with a scute length of 10.5 mm. Thus, there seems to be a negative allometry with respect to standard length.

### *Lepidotrichia*

All specimens, show lepidotrichia in all fins. In small individuals, lepidotrichia are unsegmented and unbranched (see Fig. 10D). First evidences of branching are visible in a 41.8 mm long specimen (MHNM 06-90). At a length of 102.3 mm (FMNH UC 2127, Fig. 10A), the first evidences of segmentation appear; only the proximal ends of some lepidotrichia have segments of ca. 1 mm long, the distal four-fifth is unsegmented. Branching goes up to a third order and is present only in the distal third of the lepidotrichia. In a larger specimen (FMNH UF 45, ca. 252 mm; Fig. 10B), branching is visible in both the unsegmented and segmented parts of lepidotrichia of the anal fin. This branching goes up to a fourth order. The segmented area extends distally up to half-length of the fin for

lepidotrichia at the anterior border of the fin, whereas it spreads only to a fifth of the length for the posterior ones. The largest lepidotrichia segments are ca. 2 mm long.

### ***Ontogenetic pathway***

In order to summarize the ossification pattern of *E. foordi*, an ontogenetic pathway was constructed by plotting the cumulative number of ossified elements against the standard length of specimens (Fig. 11). The pathway was constructed based on 481 elements (seven in each pectoral, seven in each pelvic, four in the first dorsal, six in the second dorsal, six in the anal, 266 in the vertebral column, and 171 in the caudal fin) counted in 65 specimens. For all paired elements, when one of them was visible on one side, the complementary one was assumed to be present. The number of newly ossified elements takes into account the first occurrence of a bone as presented in figures 2 and 7. For each vertebral unit, at least six elements are potentially visible: two pleurocentra, two intercentra and the two halves of the neural arch/spine complex. In addition, vertebral units posterior to vertebrae 31 have the two halves of the haemal arch/spine complex. In the caudal fin, vertebral units posterior to vertebrae 41 also have one ventral caudal radial. Ribs were not taken into account in our study.

In the paired fins, all radials elements were counted as a single structure. All the structures seen in one fin were considered to be also present in the opposite fin, even if not visible. The pectoral fin comprises a humerus, an ulna, a radius and a group of radials. Similarly, the pelvic fin is composed of a pelvic basal element (pelvic girdle), a femur, a tibia, a fibula and a group of radials. Unpaired fins are constituted of one basal plate and

from one to three radials; one in the first dorsal fin and three in both the second dorsal and the anal fins. Each of the seven fins (not including the caudal fin) possesses a basal scute on both sides of the fish.

Ontogeny is a continuous sequence of relatively long stabilized states or steps, alternating with short less stable intervals or thresholds (Hensel, 1999: p.277). Six distinct periods (three steps and three thresholds) can be distinguished during the stepwise ontogenetic pathway of *E. foordi* (numbered 1 to 6 in Fig. 11) ranging in standard length from 27.0 mm to 270.6 mm. The pathway is divided based solely on visual breaks in the tempo; for each period, a rate of ossification is calculated. The ossification rate corresponds to the number of elements that ossify during a period. The rate is given in terms of number of bones per millimetre of growth.

During the first step of the pathway (from 27 to 42 mm in standard length), only two neural spines and the cleithra were ossified in *E. foordi*. During this period, the ossification rate was low, at 0.14 elements/mm. The first threshold occurred between 42 and 54 mm, while the rate of ossification rose to 3.92 elements/mm. It corresponds to the settlement of the bones of the posterior part of the body, in the second dorsal, anal and caudal fins. This threshold was followed by a long period of gradual events, from 54 to 160 mm in standard length, during which the ossification rate dropped to 0.58 element/mm. The second threshold occurred between 160 and 177 mm. It corresponds to the most rapid development, reaching a rate of 9.33 elements/mm. This threshold is associated with the settlement of the anterior part of the vertebral column. Between 177 and 247 mm in standard length, a relatively calm period constitutes the pathway where the ossification rate

dropped to 0.29 element/mm. Finally, from a standard length of 247 mm, ossification events accumulate more gradually than during the two previous developmental thresholds, at a rate of 2.03 elements/mm.

Our largest specimen was 270.6 mm long in standard length, but the sequence of ossification of *E. foordi* does not stop at that point. Numerous bony elements of the vertebral column are still to appear, especially the pleurocentra of the posterior half of the body (more than 25 vertebral units do not display it in the entire sample). In the last three centimetres of growth, most of the pleurocentra of the anterior half appear relatively suddenly (Fig. 7). We can suppose that the shape of the graphic (Fig. 11) would continue in a threshold if our sample had comprised larger specimens.

## DISCUSSION

The ontogeny of *E. foordi* had been studied morphometrically (Thomson and Hahn, 1968; Schultze, 1984) and in term of coarse sequence of ossification (Cote et al., 2002), but these works lack a temporal dimension. Our results provide information about the rates of development, revealing variable ossification rates in this organism.

The hypothesis of saltatory ontogeny, as documented by Balon (1979, 1984, 1986), stipulates that development does not proceed by a continuous accumulation of inconspicuous, small changes but is a sequence of rapid changes in form and function alternating with prolonged intervals (steady states) of slower development. The ontogenetic pathway of *Eusthenopteron foordi* based on the ossification pattern shows an obvious saltatory development with three distinct thresholds.

The first one, at a standard length of ca. 50 mm represents the settlement of the structures of the posterior part of the body: last neural spines and ventral caudal radials in the caudal fin, distal elements in the second dorsal and the anal fins. The second threshold happens at a standard length of ca. 160 mm and corresponds to the rapid ossification of the vertebral elements in the anterior part of the body. Between those thresholds, most of the fins gradually ossify the more proximal bones of their structure. The ontogenetic pathway is not associated with any changes in body proportions, as Schultze (1984) demonstrated the absence of variation in the proportions of the postcranial skeleton during growth.

Saltatory ontogeny has been reported, among others, for the cyprinid *Leucaspis delineatus* (Pinder and Gozlan, 2004), *Phoxinus phoxinus* (Predrag et al. 1999), *Abramis ballerus* (Balon, 1959) and *Chondrostoma toxostoma* (Gozlan et al., 1999), for the percid *Etheostoma caeruleum* (Paine and Balon, 1984), for the catostomid *Catostomus commersoni* (McElman and Balon, 1980), and for the balitorid *Barbatula barbatula* (Kováč et al., 1999). Saltatory patterns implied anatomical systems (e.g., circulatory system, shape of the tail) and behavioural characteristics (e.g., alimentary changes). For instance, Sakakura and Tsukamoto (1999) demonstrated that ontogenetic changes can have direct influence on the behaviour of the carangid *Seriola quinqueradiata*. The relatively rapid ossification of the vertebrae is correlated in *S. quinqueradiata* with an increase in tissue cortisol level, the latter being responsible of an onset in aggressive behaviour.

It is not possible to correlate the changes in development rates of *Eusthenopteron* ontogeny with any change in body proportion. We can only assess, as did Cote et al. (2002), that these ontogenetic changes were probably linked to behavioural changes, which

therefore may have resulted in changes in habitat use. The first threshold allows the appearance of propulsive structures (anal and second dorsal fins), while stabilising structures (paired fins) are formed during the second threshold. Parent and Cloutier (1996) did not find a correlation between the size of the specimens and the type of sediments in which they are preserved. Thus, there is no evidence for habitat selection in relation to the facies. We hypothesize that *E. foordi* already had to perform rapid accelerations at the beginning of its life (as did the adults; Belles-Isles, 1992), as suggested by the early ossification of all the propulsive apparatus (caudal, anal and second dorsal fins).

Most bones in the skull of *Eusthenopteron foordi* ossified at an early ontogenetic stage. This advanced ossification in the head region, including ossification of branchial arches, provided jaw dynamic possibilities (like the suction feeding mode performed by the adults; Thomson, 1967), revealing the necessity of preying at the first days of life in *Eusthenopteron*. Even the smallest individuals were free-feeding organisms, as revealed by the absence of any trace of vitellus sac. This concurs with the early ossification of the posterior part of the body, allowing a powerful propulsive thrust related to predatory skills.

Mabee et al. (2002) observed consistent patterns in the development of median fins in all living actinopterygians, and they interpret these patterns as evidence of developmental modularity. These patterns are: (1) primitive symmetry of dorsal and anal fins position along the anterior to posterior axis, (2) co-differentiation of dorsal and anal fins, and (3) shared directions of differentiation of exoskeletal fin rays and endoskeletal supports in all fins. Our work proves that the establishment of the sequence of ossification can lead to the study of modularity in a fossil species. *Eusthenopteron foordi* displays a

positioned symmetry of the second dorsal and anal fin, both fins being inserted at the level of the same vertebra, the number 37. Both fins also have the same isometric growth and progress along the body axis at the same rate during overall growth. It coincides with the Dorsal+Anal Fin Positioning Module of Mabee et al. (2002). The second dorsal and anal fins of *E. foordi* also undergo ossification at the same moment, at a length of 44.5 mm (MHNM 06-535), and their respective pattern of ossification are fairly the same. Skeletal elements of the second dorsal and anal fins differentiate in a similar distal-proximal manner, thus fitting the Dorsal+Anal Fin Patterning Module of Mabee et al. (2002). However, the postero-anterior direction of the second dorsal fin is not repeated in the anal fin. Positioning and patterning modules in the median fins of the Devonian sarcopterygian *E. foordi* are similar to those found in living actinopterygians. Furthermore, actinopterygian hypurals develop bidirectionally (Mabee et al., 2002) and similarly, haemal spines of the caudal fin of *E. foordi* also developed bidirectionally.

In *Eusthenopteron*, similar patterns of ossification are present in different fins. All fins but the caudal show distal elements to be ossified earlier than proximal elements. This distal-proximal ossification of paired fins differs from those of tetrapods (Schmalhausen, 1917; Shubin and Alberch, 1986) and dipnoans (Arratia et al., 2001). It is interesting to note that middle elements of the pelvic fins (tibia) and middle elements of the pectoral fins (radius and ulna) are visible for the first time in the same specimen, CMN 52263 (S.L.: 118.2 mm). The simultaneous appearance of these homologous structures points toward a relative importance of the fin manoeuvrability between 50 and 150 mm of standard length (step no. 3 in Fig. 11).

The index of reliability suggests that the ossification pattern of the second dorsal and anal fins is the most accurate whereas that of the pectoral and pelvic fins is less reliable. This could also suggest that the pattern of paired fins is more variable than that of the unpaired fins or that it is more similar taphonomically. The last hypothesis implies a greater similarity in terms of endochondral ossification among paired fins.

Basal scutes are among the first elements to ossify for each fin with the exception of the anal fin. Furthermore, basal scutes possess the lowest reliability index and the largest gap for the sequence in each fin. Basal scutes have been mainly observed in small individuals. This bias could be related to the fragile nature of those thin plates; exceptional conditions are required to preserve them. Delicate and poorly ossified small specimens required also extremely good preservation conditions to be fossilized. Conditions good enough to preserve small individuals, will favour the preservation of basal scutes. Larger specimens, with well developed bony structures can be preserved in relatively less favourable conditions of fossilisation. However, these poorer conditions are not sufficient to preserve basal scutes.

## CONCLUSION

The study of the size series of *Eusthenopteron foordi* confirms isometric growth in this species. Complete sequence of ossification of *E. foordi* provides the first empirical example of saltatory ontogeny in the fossil record. Reliability indices (RI) were calculated and demonstrated that this growth series is highly reliable for the second dorsal and anal fins, the other fin systems displaying lower RI's. The overall sequence is relatively

reliable, but the low RI's and the large gaps in the sequence recall us to be particularly careful in our interpretations. Second dorsal and anal fins having symmetric positioning along the anterior to posterior axis and differentiating in a similar manner during growth, it proposes evidence of developmental modularity of this extinct species and reveals consistencies in development of actinopterygians and sarcopterygians. The pattern of ossification of at least these two median fins was obviously inherited from a common osteichthyan ancestor.

## **ACKNOWLEDGMENTS**

The authors are deeply grateful to John Maisey and Ivy Rutzsky at the American Museum of Natural History (New York); to Stephen Cumbaa, Kieran Shepherd and Elizabeth Feuerstach at the Canadian Museum of Nature (Ottawa); to Lance Grande and Elaine Zeiger at the Field Museum of Natural History (Chicago); and to Sylvain Desbiens, Johanne Kerr and Norman Parent at the Musée d'Histoire Naturelle de Miguasha, for advices and friendly welcoming in their respective institutions. We also thank André Lévesque at Université Laval (Québec City) and Robert L. Carroll at McGill University (Montréal) for the loan of specimens. This research was supported by the Thomas J. Dee Fellowship Fund (FMNH), the Collection Study Grant Fund (AMNH), the Natural Sciences and Engineering Research Council of Canada (NSERC research grant to Richard Cloutier, 238612) and the Fondation Gérard D. Lévesque. Jean Ferron and Hans Larsson commented earlier versions of the manuscript.

**REFERENCES**

- Andrews, S. M. and T. S. Westoll. 1970. The postcranial skeleton of *Eusthenopteron foordi* Whiteaves. Transactions of the Royal Society of Edinburgh 68:207-329.
- Arratia, G., H.-P. Schultze and J. Casciotta. 2001. Vertebral column and associated elements in dipnoans and comparison with other fishes: development and homology. Journal of Morphology 250:101-172.
- Balon, K. E. 1959. Die embryonale und larvale Entwicklung der Donauzope (*Abramis ballerus* subsp.). Biologické práce 5:1-87.
- Balon, E. K. 1979. The theory of saltation and its application in the ontogeny of fishes: steps and thresholds. Environmental Biology of Fishes 4:97-101.
- Balon, E. K. 1984. Reflections on some decisive events in the early life of fishes. Transactions of the American Fisheries Society 113:178-185.
- Balon, E. K. 1986. Saltatory ontogeny and evolution. Rivista di Biologia/Biology Forum 79:151-190.
- Balon, E. K. 1999. Alternative ways to become a juvenile or a definitive phenotype (and on some persisting linguistic offences). Environmental Biology of Fishes 56:17-38.
- Belles-Isles, M. 1992. The modes of swimming of sarcopterygians. pp. 117-130 in E. Mark-Kurik (ed.), Fossil fishes as living animals. Academy of Sciences of Estonia, Tallinn.
- Carroll, R. L., A. Kuntz and K. Albright. 1999. Vertebral development and amphibian evolution. Evolution and Development 1:36-48.

- Chipman, A. D., and E. Tchernov. 2002. Ancient ontogenies: larval development of the Lower Cretaceous anuran *Shomronella jordanica* (Amphibia: Pipoidae). *Evolution and Development* 4:86-95.
- Cloutier, R. 1996. Taxonomic review of *Eusthenopteron foordi*. pp. 271-284 in H.-P. Schultze and R. Cloutier (eds), *Devonian Fishes and Plants of Miguasha, Quebec, Canada*. Verlag Dr. Friedrich Pfeil, München.
- Cloutier, R. 1997. Morphologie et variations du toit crânien du dipneuste *Scaumenacia curta* (Whiteaves) (Sarcopterygii), du Dévonien supérieur du Québec. *Geodiversitas* 19(1):61-105.
- Cloutier, R., and P. E. Ahlberg. 1996. Morphology, characters and interrelationships of basal sarcopterygians. pp. 445-479 in M. L. J. Stiassny, L. R. Parenti and G. D. Johnson (eds), *Interrelationships of Fishes*. Academic Press, New York.
- Cloutier, R., S. Loboziak, A.-M. Candilier and A. Blicek. 1997. Biostratigraphy of the Upper Devonian Escuminac Formation, Eastern Quebec, Canada: a comparative study based on miospores and fishes. *Review of Palaeobotany and Palynology* 93:191-215.
- Cote, S., R. Carroll, R. Cloutier, and L. Bar-Sagi. 2002. Vertebral development in the Devonian sarcopterygian fish *Eusthenopteron foordi* and the polarity of vertebral evolution in non-amniote tetrapods. *Journal of Vertebrate Paleontology* 22:487-502.
- Gozlan, R. E., G. H. Copp and J.-N. Tourenq. 1999. Early development of the sofie, *Chondrostoma toxostoma*. *Environmental Biology of Fishes* 56:67-77.

- Grünbaum, T., R. Cloutier and P. Dumont. 2003. Congruence between chondrification and ossification sequences during caudal skeleton development: a Moxostomatini case study. pp. 161-176 in H. I. Browman and A. B. Skiftesvik (eds), *The Big Fish Bang: Proceedings of the 26<sup>th</sup> Annual Larval Fish Conference*, Bergen, Norway.
- Hensel, K. 1999. To be a juvenile and not to be a larva: an attempt to synthesize. *Environmental Biology of Fishes* 56:277-280.
- Jolicoeur, P. 1968. Interval estimation of the slope of the major axis of a bivariate normal distribution in the case of a small sample. *Biometrics* 24:679-682.
- Kováč, V., G. H. Copp and M. P. Francis. 1999. Morphometry of the stone loach, *Barbatula barbatula*: do mensural characters reflect the species' life history thresholds? *Environmental Biology of Fishes* 56:105-115.
- Mabee, P. M., P. L. Crotwell, N. C. Bird and A. C. Burke. 2002. Evolution of median fin modules in the axial skeleton of fishes. *Journal of Experimental Zoology* 294:77-90.
- Mabee, P. M., K. L. Olmstead and C. C. Cabbage. 2000. An experimental study of intraspecific variation, developmental timing and heterochrony in fishes. *Evolution* 54:2091-2106.
- Mabee, P. M. and T. A. Trendler. 1996. Development of the cranium and paired fins in *Betta splendens* (Teleostei: Percomorpha): intraspecific variation and interspecific comparisons. *Journal of Morphology* 227:249-287.
- Maisano, J. A. 2002. The potential utility of postnatal skeletal developmental patterns in squamate phylogenetics. *Zoological Journal of the Linnean Society* 136:277-313.

- McElman, J. F. and E. K. Balon. 1980. Early ontogeny of white sucker, *Catostomus commersoni*, with steps of saltatory development. *Environmental Biology of Fishes* 5:191-224.
- Paine, M. D. and E. K. Balon. 1984. Early development of the rainbow darter, *Etheostoma caeruleum*, according to the theory of saltatory ontogeny. *Environmental Biology of Fishes* 11:277-299.
- Parent, N. and R. Cloutier. 1996. Distribution and preservation of fossils in the Escuminac Formation. pp. 54-78 in H.-P. Schultze and R. Cloutier (eds), *Devonian Fishes and Plants of Miguasha, Quebec, Canada*. Verlag Dr. Friedrich Pfeil, München.
- Pinder, A. C. and R. E. Gozlan. 2004. Early ontogeny of sunbleak. *Journal of Fish Biology* 64:762-775.
- Predrag, D. S., P. Garner, E. A. Eastwood, V. Kováč and G. H. Copp. 1999. Correspondence between ontogenetic shifts in morphology and habitat use in minnow *Phoxinus phoxinus*. *Environmental Biology of Fishes* 56:117-128.
- Sakakura, Y. and K. Tsukamoto. 1999. Ontogeny of aggressive behaviour in schools of yellowtail, *Seriola quinqueradiata*. *Environmental Biology of Fishes* 56:231-242.
- Schmalhausen, I. 1917. On the extremities of *Ranidens sibiricus* Kessl. *Revue Zoologique Russe* 2:129-135.
- Schultze, H.-P. 1984. Juvenile specimens of *Eusthenopteron foordi* Whiteaves, 1881 (osteolepiform rhipidistian, Pisces) from the Late Devonian of Miguasha, Quebec, Canada. *Journal of Vertebrate Paleontology* 4:1-16.

- Schultze, H.-P. and D. Bardack. 1987. Diversity and size changes in paleonisciform fishes (Actinopterygii, Pisces) from the Pennsylvanian Mazon Creek Fauna, Illinois, U.S.A. *Journal of Vertebrate Paleontology* 7(1):1-23.
- Shubin, N. H. and P. Alberch. 1986. A morphometric approach to the origin and basic organisation of the tetrapod limb. *Evolutionary Biology* 1:319-387.
- Stensiö, E. A. 1925. Note on the caudal fin of *Eusthenopteron*. *Arkiv Zoologisk* (Stockholm) 17B:1-3.
- Thomson, K. S. 1967. Mechanisms of intracranial kinetics in fossil rhipidistian fishes (Crossopterygii) and their relatives. *Zoological Journal of the Linnean Society* 46, 310:223-253.
- Thomson, K. S., and K. V. Hahn. 1968. Growth and form in fossil rhipidistian fishes (Crossopterygii). *Journal of Zoology (London)* 156:199-223.
- Weems, R. E. 2004. *Bothriolepis virginiensis*, a valid species of placoderm fish separable from *Bothriolepis nitida*. *Journal of Vertebrate Paleontology* 24(1):245-250.
- Werdelin, L. and J. A. Long. 1986. Allometry in the placoderm *Bothriolepis canadensis* and its significance to antiarch evolution. *Lethaia* 19:161-169.
- Zhu, M. and H.-P. Schultze. 2001. Interrelationships of basal osteichthyans. pp. 289-314 in P. E. Ahlberg (ed.), Major events in early vertebrate evolution. Paleontology, phylogeny, genetics and development. Systematics Association Special Volume Series 61. Taylor and Francis, London and New York.

**Table 1** Major axis and 95% confidence interval for the slope for six fin position in relation to the standard length of *Eusthenopteron foordi* ( $x = \log_{10}$  transformed data,  $y = \log_{10}$  transformed standard length). These equations correspond to the scatter plots of figure 3.

Graph	Major axis	95% Confidence interval for the slope
Operculum-First dorsal fin (N=19; Fig. 3A)	$y = 0.816x + 0.078$	[0.8695; 1.308]
Operculum-Second dorsal fin (N=20; Fig. 3B)	$y = 0.899x + 0.127$	[0.857; 1.222]
Operculum-Pelvic fin (N=17; Fig. 3C)	$y = 0.833x - 0.005$	[0.826; 1.278]
Operculum-Anal fin (N= 20; Fig. 3D)	$y = 0.917 + 0.061$	[0.863; 1.222]
Operculum-Upper caudal fin (N=20; Fig. 3E)	$y = 0.937x - 0.001$	[0.868; 1.238]
Operculum-Lower caudal fin (N=19; Fig. 3F)	$y = 0.947x - 0.031$	[0.851; 1.237]

**Table 2** Ossification sequence reliability for each appendicular skeleton structure for 56 *Eusthenopteron foordi*. See explanations in the text for the definition and interpretation of the parameters.

Fin	Structure	Number of specimens		Reliability index	Gap		
		Actual	Expected		Specimens	Length (mm)	Position
Pectoral	Cleithrum	26	56	0.46	5	37.3	Mid-Early
	Humerus	7	23	0.30	8	58.4	Mid-Late
	Ulna	9	29	0.31	6	45.1	Medium
	Radius	12	29	0.41	5	39.8	Medium
	Radials	11	39	0.28	5	46.3	Mid-Late
	Basal scutes	5	48	0.10	9	51.3	Medium
Pelvic					15	83.4	Medium
					15	86.8	Late
	Girdle	11	22	0.50	3	14.2	Late
	Femur	7	20	0.35	7	33.4	Mid-Late
	Tibia	11	34	0.32	7	39.8	Medium
	Fibula	8	25	0.32	8	39.0	Mid-Late
First dorsal	Radials	7	37	0.19	11	61.9	Mid-Late
	Basal scutes	7	55	0.13	16	60.5	Early
	Basal plate	19	39	0.49	3	28.9	Medium
	Radial	18	48	0.38	15	68.7	Mid-Early
	Basal scutes				8	49.2	Mid-Early
					8	35.4	Medium
Second dorsal	Basal plate	30	41	0.73	4	18.5	Medium
	Radial 1	42	56	0.75	5	16.5	Mid-Early
	Radial 2	45	59	0.76	5	16.5	Mid-Early
	Radial 3	40	59	0.68	3	6.1	Mid-Early
	Basal scutes	12	60	0.20	10	33.4	Late
Anal	Basal plate	33	39	0.85	2	7.9	Medium
	Radial 1	40	57	0.70	4	7.6	Mid-Early
	Radial 2	44	57	0.77	6	10.8	Mid-Early
	Radial 3	41	57	0.72	5	15.1	Early
	Basal scutes	14	55	0.25	9	52.7	Medium

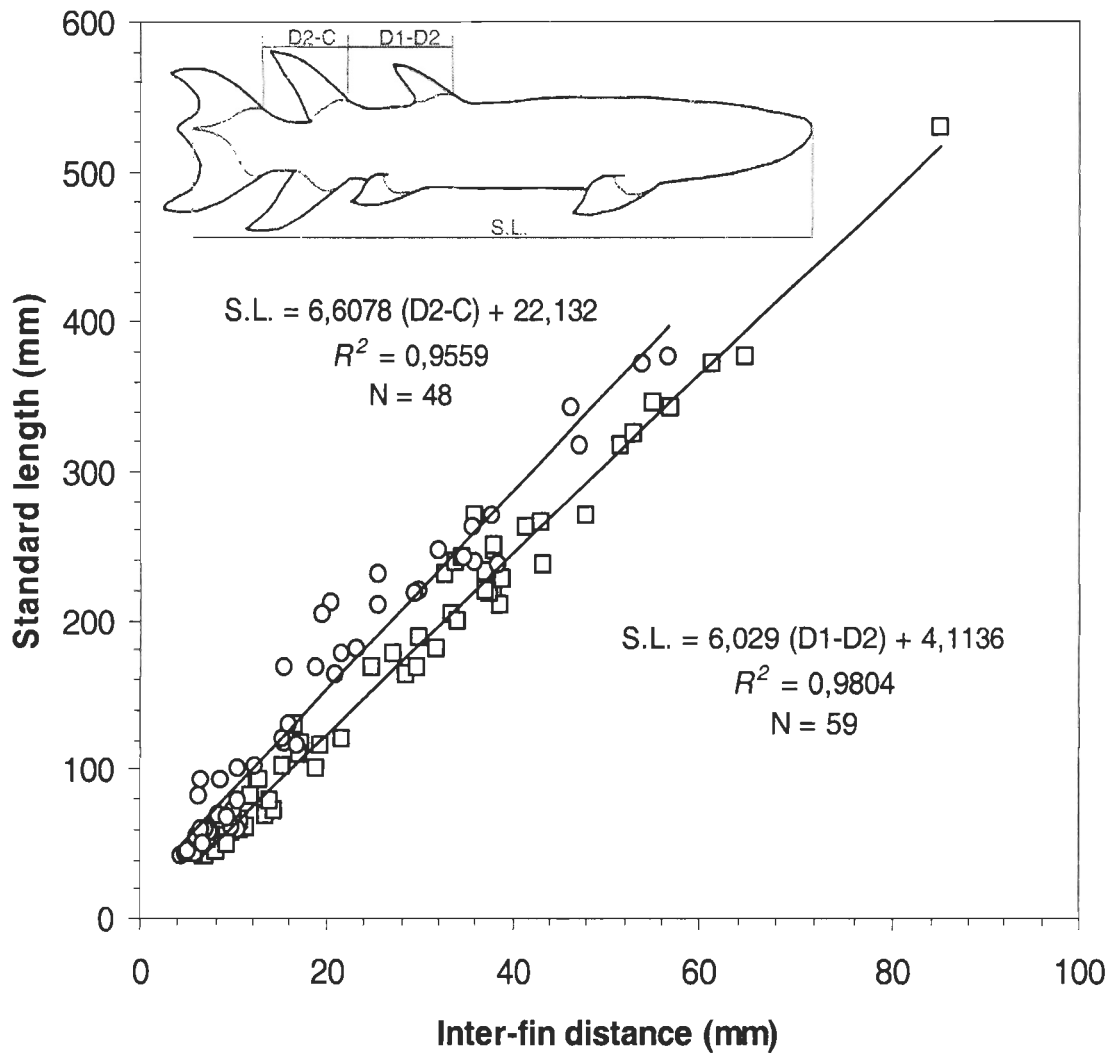
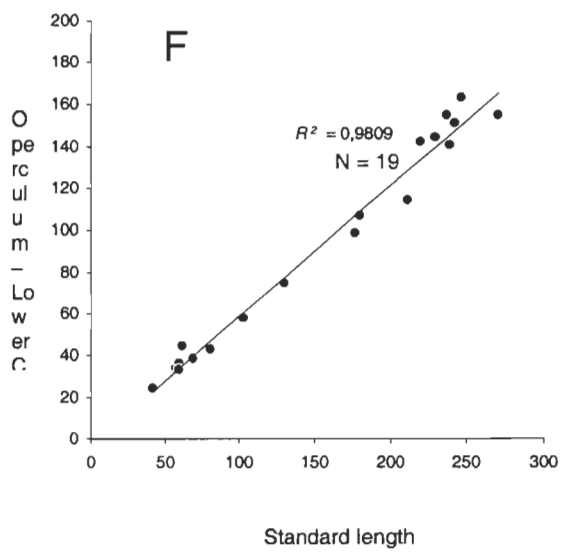
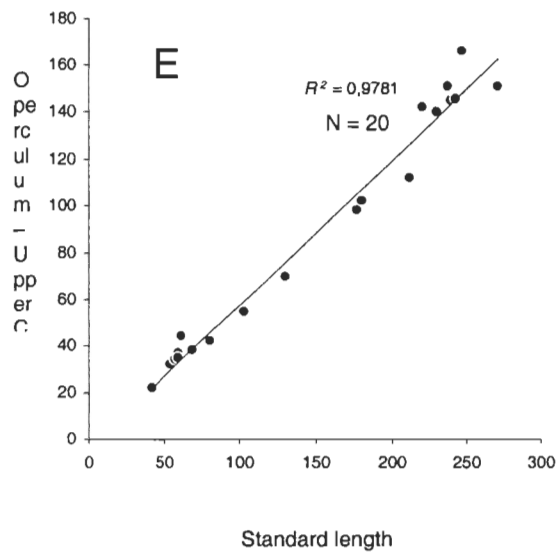
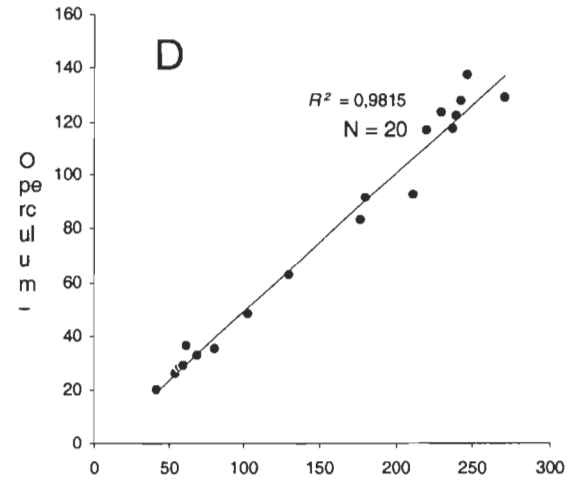
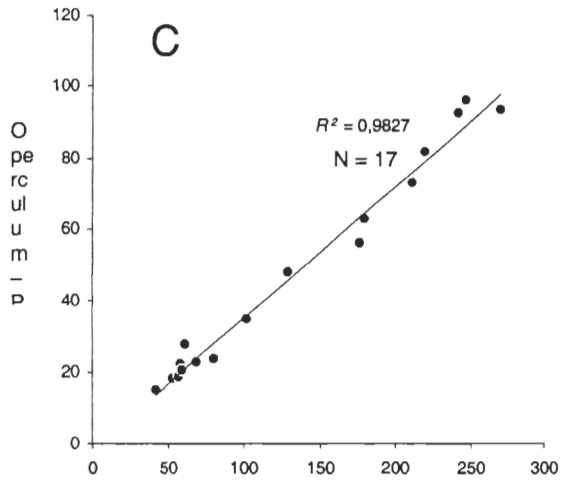
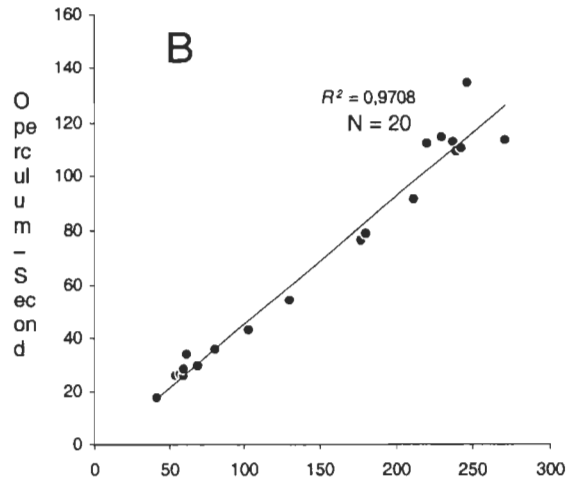
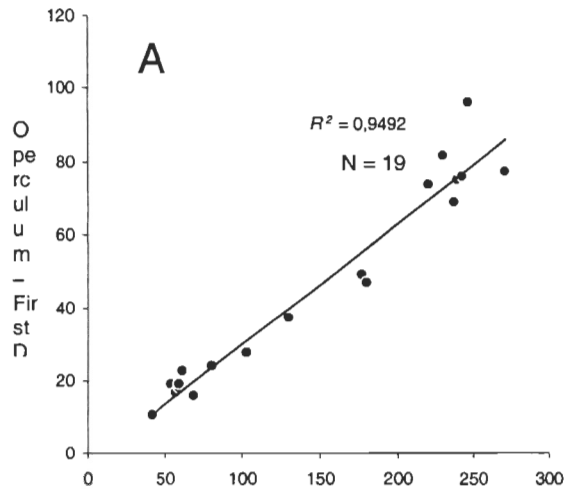


**Figure 1.** Scatter diagram of standard length (mm) plotted against distance (mm) between insertion points of fins in *Eusthenopteron foordi*. The lower regression line ( ) corresponds to the distance between insertion points of the first and second dorsal fins (D1-D2); the upper regression line ( ) corresponds to the distance between the insertion point of the second dorsal fin and the insertion point of the epichordal lobe of the caudal fin (D2-C). Data were obtained from Thomson and Hahn (1968), Schultze (1984), and original measurements.

**Figure 2.** Sequence of ossification of *Eusthenopteron foordi* for the pectoral, pelvic, dorsal and anal fins. Observed skeletal elements (dark rectangles) are recorded for 65 specimens. For each specimen, the standard length (S.L.) is given; a star indicates an estimated length according to the formulas given in the text. The light grey areas correspond to missing parts owing to partial preservation of fossils. A and B designate part and counterpart of a specimen. **Bas.:** basal plate; **Clei.:** cleithrum; **Fem.:** femur; **Fib.:** fibula; **Hum.:** humerus; **R1, R2** and **R3:** first, second and third radial in an anterior to posterior position; **Rad/Rads.:** radial/radials; **Scut.:** basal scutes.



**Figure 3.** Scatter diagrams of body measurements (mm) versus standard length (mm) in *Eusthenopteron foordi*. **A**, Distance from posterior margin of the operculum to the insertion of the first dorsal fin; **B**, distance from posterior margin of the operculum to the insertion of the second dorsal fin; **C**, distance from posterior margin of the operculum to the insertion of the pelvic fins; **D**, distance from posterior margin of the operculum to the insertion of the anal fin; **E**, distance from posterior margin of the operculum to the insertion of the epichordal lobe of the caudal fin; **F**, distance from posterior margin of the operculum to the insertion of the hypochordal lobe of the caudal fin. Regression lines are illustrated.



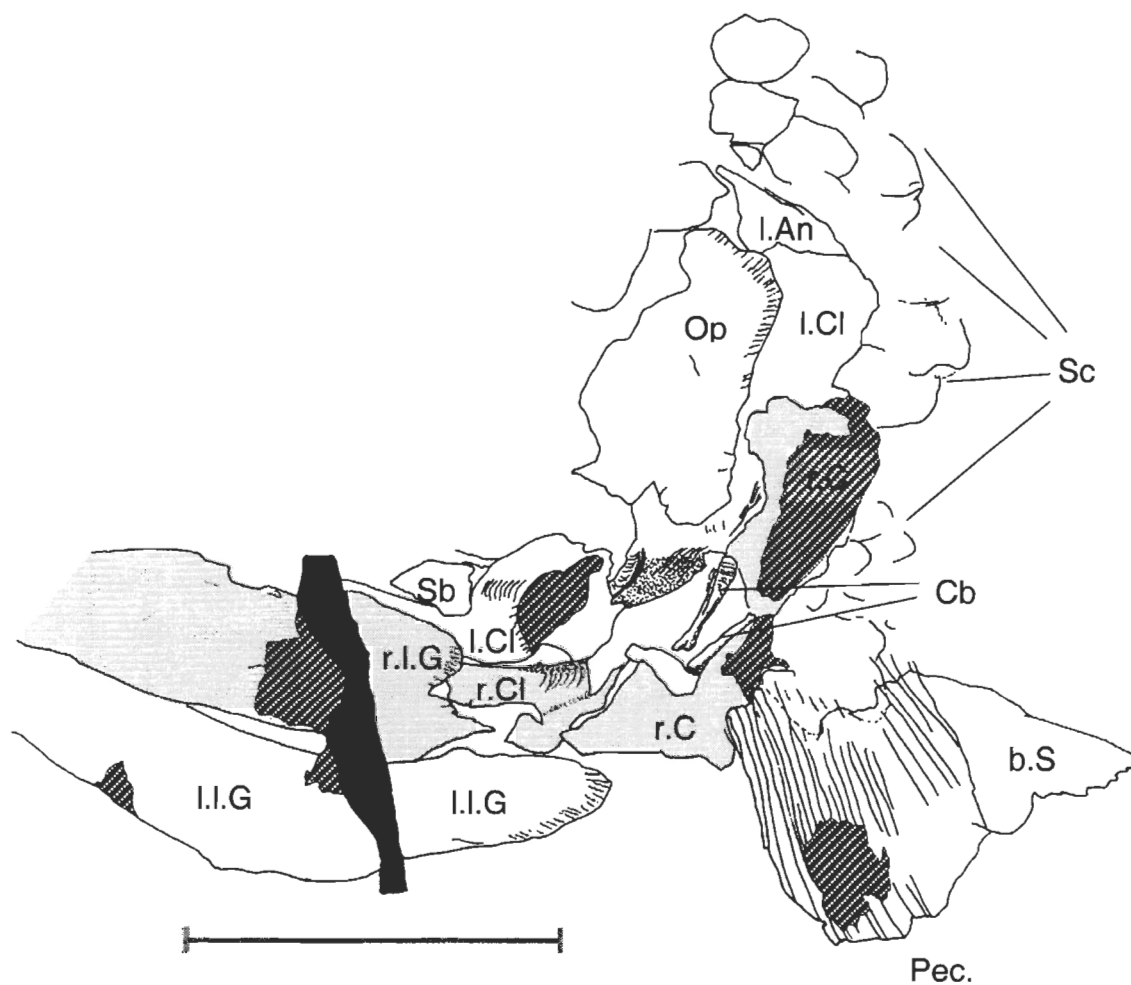


**Figure 4.** Small specimen of *Eusthenopteron foordi* (UL 265). Enlarged view of the pectoral girdle region, showing the first ossified branchial elements. **b.sc.:** basal scute; **Cbr.:** ceratobranchials; **Dt.:** dentary; **I.Ano.:** anocleithrum; **I.Cl.:** left cleithrum; **I.Cla.:** left clavicle; **I.I.Gu.:** left lateral gular plate; **Op.:** opercular; **pec.f.:** pectoral fin; **r.Cl.:** right cleithrum; **r.Cla.:** right clavicle; **r.I.Gu.:** right lateral gular plate; **sbm.:** submandibular; **Sc.:** scales. Scale bar equal 5 mm.

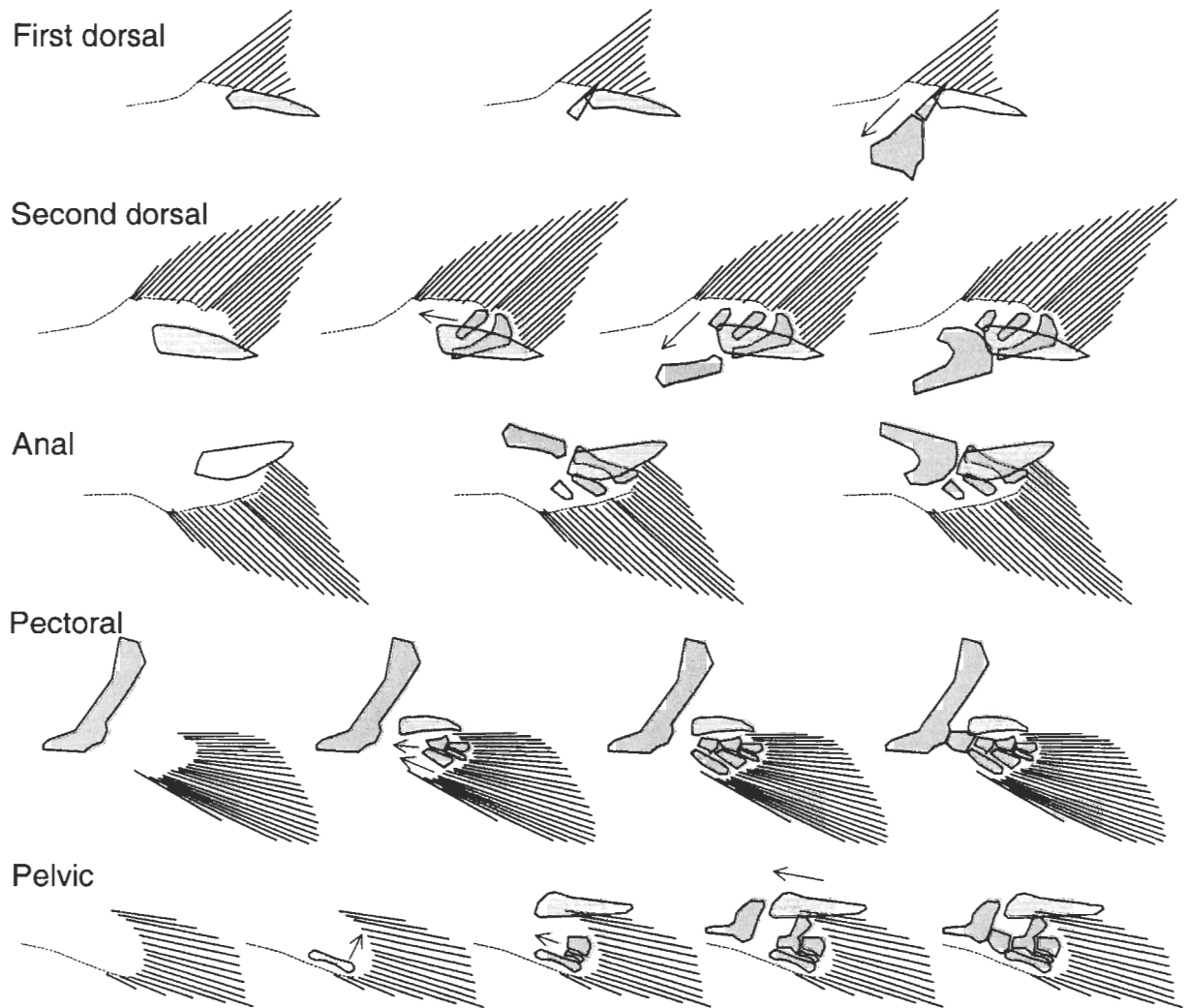
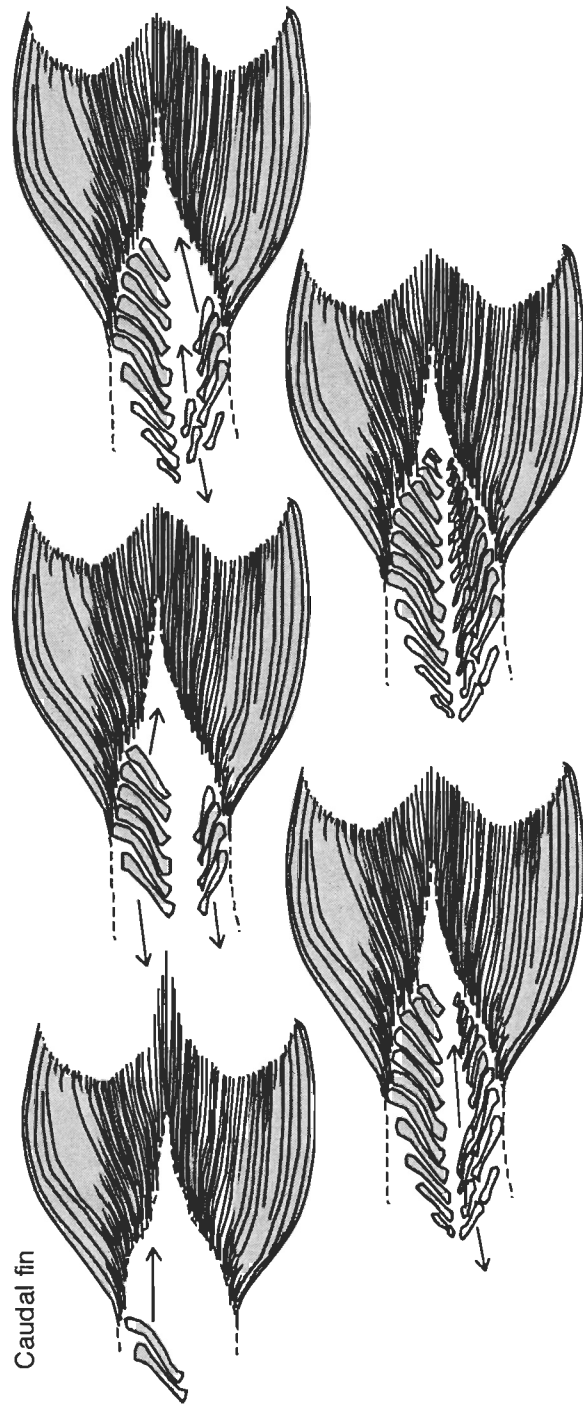


**Figure 5.** Schematic representation of the ossification of each fin in *Eusthenopteron foordi*. Stages are progressive from left to right. Solid lines correspond to fin rays, dark grey elements are endochondral bony structures and light grey elements are basal scutes. Arrows indicate direction of ossification.



Caudal fin

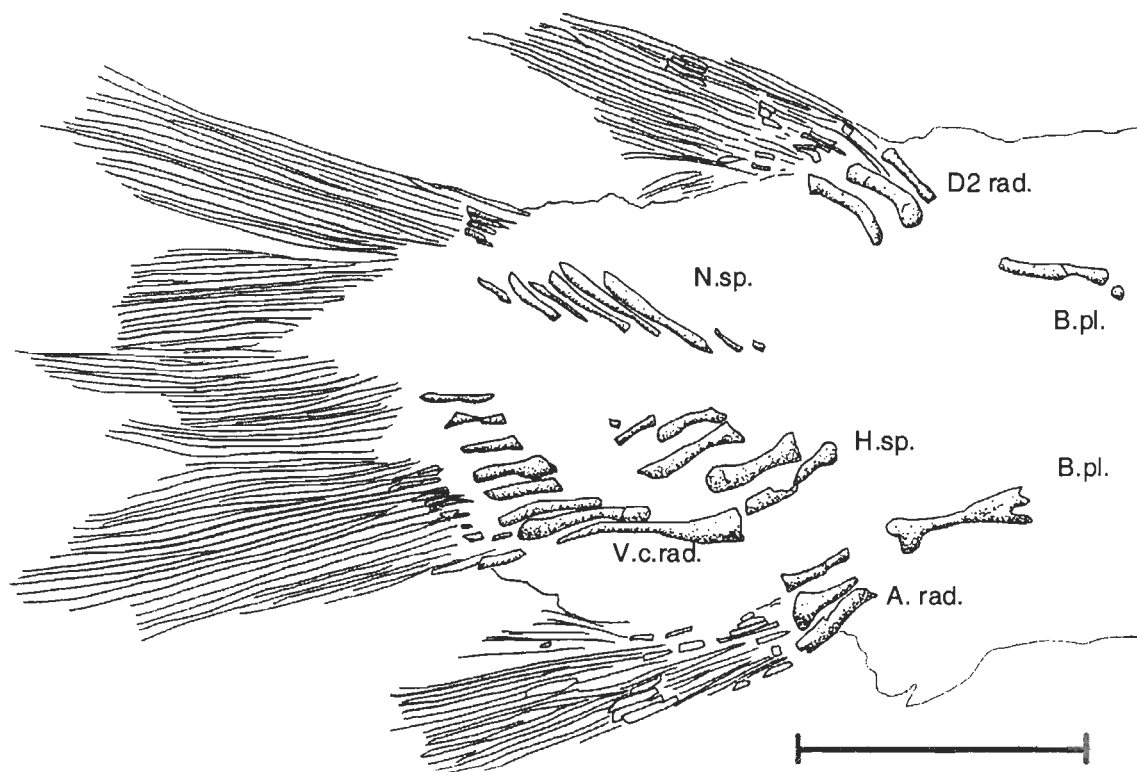


**Figure 6.** Caudal region of *Eusthenopteron foordi*, specimen MHNM 06-59 (S.L. ca. 111 mm). Rod-shaped basal elements in both the second dorsal fin and the anal fin in early stage of development. **A. rad.:** anal fin radials; **b.pl.:** basal plate; **D2 rad.:** second dorsal fin radials; **H.sp.:** haemal spines; **N.sp.:** neural spines; **V.c.rad.:** ventral caudal radials. Scale bar equals 10 mm.





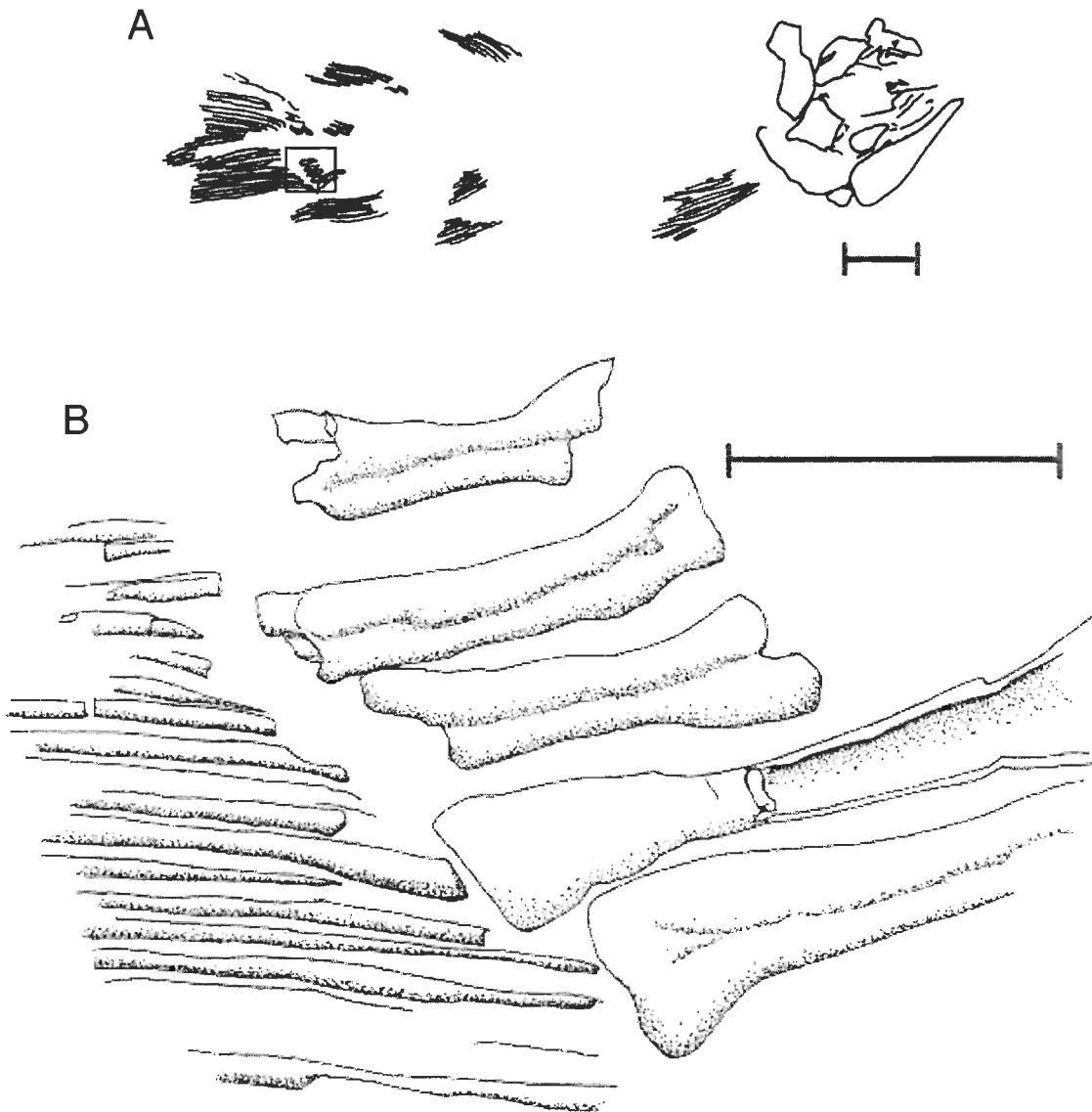


**Figure 8.** Specimen of *Eusthenopteron foordi* (UL 95, S.L.: 59.9 mm). **A**, Complete specimen. **B**, Details of the anterior ventral radials of the caudal fin. Three of them show evidence of collapsing (longitudinal grooves) owing to taphonomic process. Scale bars equal 1 mm.

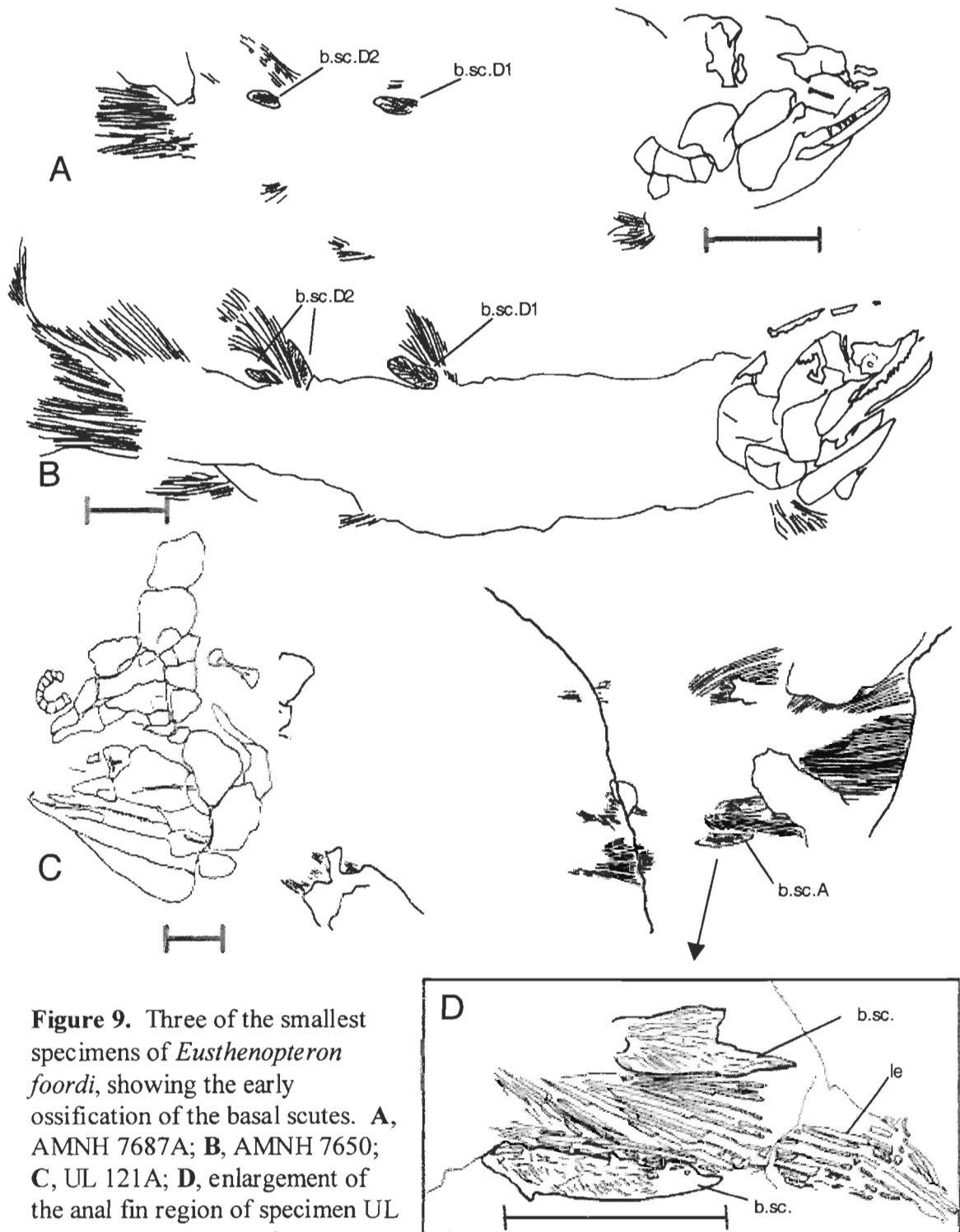


**Figure 9.** Three of the smallest specimens of *Eusthenopteron foordi*, showing the early ossification of the basal scutes. **A**, AMNH 7687A; **B**, AMNH 7650; **C**, UL 121A; **D**, enlargement of the anal fin region of specimen UL 121A. Scale bars equal 5 mm.

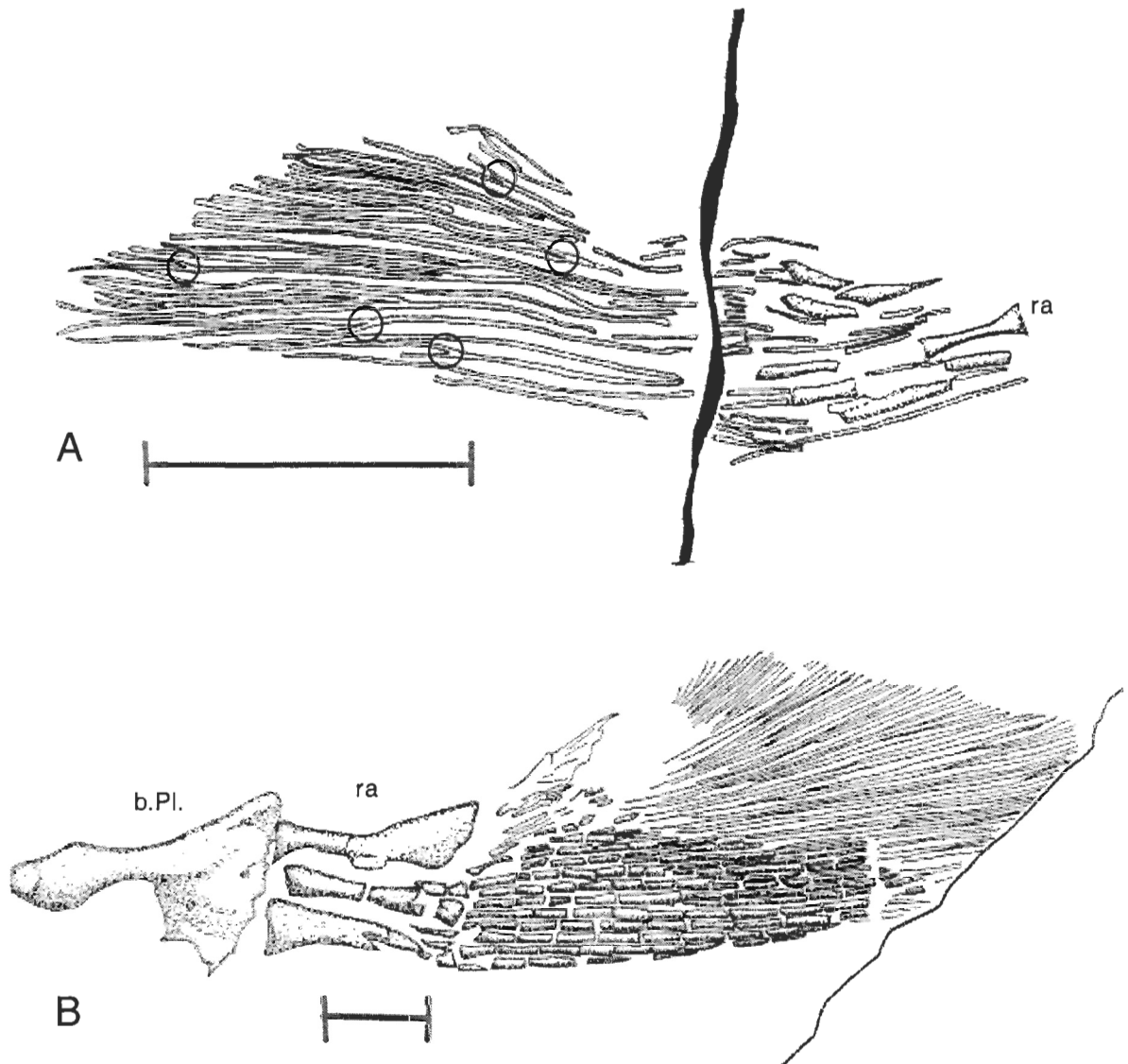


**Figure 10.** Anal fin of *Eusthenopteron foordi* showing the segmentation and branching of the lepidotrichia. Circles indicate branching. **A**, FMNH UC 2127 (S.L.: 102.3 mm); **B**, FMNH UF 45 (S.L.: ca. 252 mm). **b.Pl.:** basal plate; **ra.:** radial. Scale bars equal 5 mm.

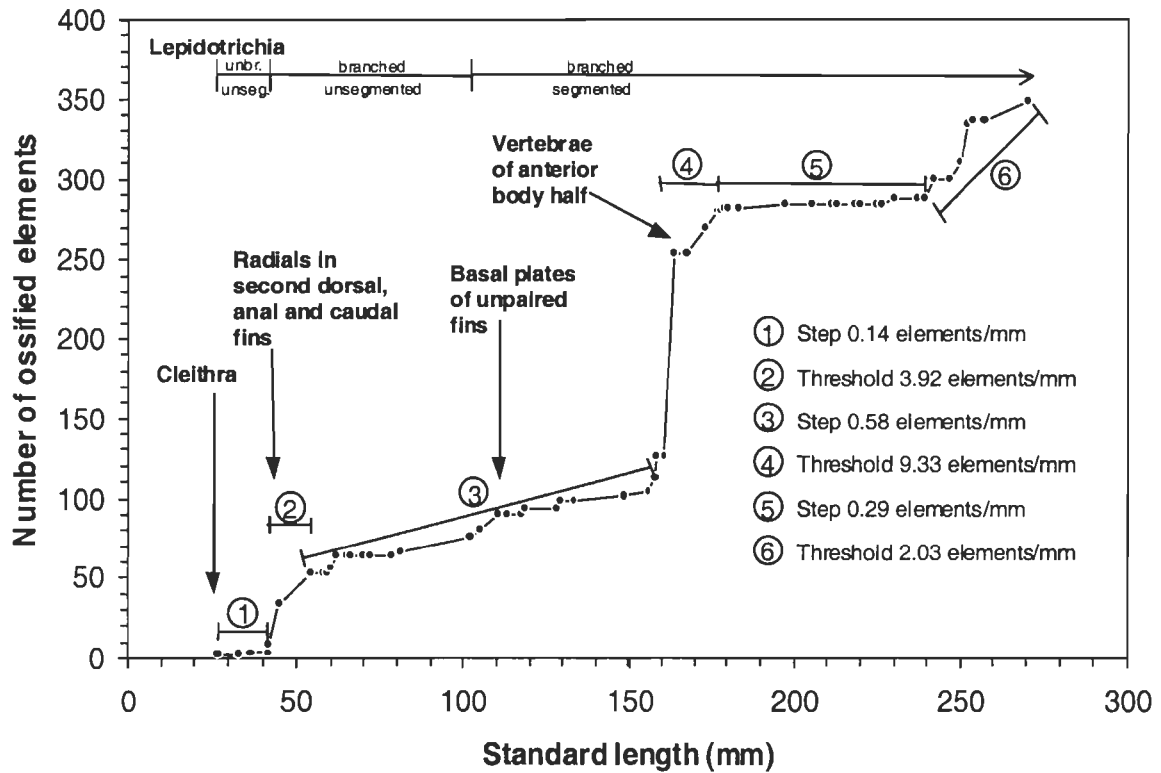


**Figure 11.** Ontogenetic pathway of *Eusthenopteron foordi*. The cumulative number of ossified elements for 65 specimens is traced against the specimen standard length. Values 1 to 6 are rate of development expressed in terms of the mean number of new elements for each millimetre of growth (elements/mm) for each step and threshold.

## CONCLUSION GÉNÉRALE

La présente recherche s'était donné comme objectif d'étudier en détails deux aspects de la biologie du poisson fossile *Eusthenopteron foordi*. Le premier concernait un débat qui dure depuis 24 ans, soit celui sur la présence ou l'absence de choanes. Nos résultats semblent clairement démontrer qu'il possédait des choanes fonctionnelles. Les images de la région nasale de trois spécimens obtenues par tomographie axiale permettent de visualiser un conduit reliant sans encombre la cavité buccale à la capsule nasale et dans lequel aucune dent de la mandibule ne vient s'insérer lors de l'occlusion. Les futures analyses phylogénétiques pourront désormais coder le caractère choane comme présent sur la base de preuves solides. Nous avons toutefois démontré que dans le cas d'analyses cladistiques précédemment publiées, le fait de coder la choane comme présente ou absente, ou même d'éliminer le caractère "choane" des matrices, n'avait qu'une influence mineure sur le nombre d'arbres également parcimonieux et la longueur de ceux-ci. La choane étant dans ces cas-là un caractère parmi de nombreux autres, son importance est avant tout conceptuelle et historique.

La suite de nos travaux aura aussi une influence sur l'élaboration des futurs arbres phylogénétiques. L'établissement de la séquence d'ossification pour tout le squelette de l'*Eusthenopteron foordi*, de même que sa trajectoire ontogénétique, ont permis de déceler un patron de croissance saltatoire chez ce poisson. Déjà étudié chez plusieurs espèces de poissons actuelles, ce type de développement est confirmé pour la première fois chez une espèce fossile. La croissance de l'*E. foordi* était caractérisée par des accélérations dans le taux d'ossification de son squelette. Vers une longueur standard d'environ 50 mm, la

majeure partie de son squelette postérieur s'ossifiait et lui conférait de bonnes aptitudes à la propulsion. Ensuite, après une relative stagnation dans le développement, une nouvelle accélération ontogénétique survenait vers une longueur standard de 160 mm et voyait la mise en place d'une grande partie des os de la partie antérieure de la colonne vertébrale.

À mesure que ce type d'étude se généralisera en paléontologie, les successions d'événements ontogénétiques pourront être utilisées en tant que caractères propres dans les analyses phylogénétiques. Le fait par exemple que toutes les nageoires démontrent une direction de développement de la partie distale vers la partie proximale pourra éventuellement servir de référence à un caractère du genre « direction ontogénétique des nageoires ». Il faudra évidemment que de nombreux efforts soient investis dans la détermination de séquences d'ossification chez d'autres espèces fossiles pour commencer à profiter de cette opportunité dans l'élaboration des cladogrammes.

Pour la première fois, des modules de développement ont été observés chez une espèce fossile. Chez l'*Eusthenopteron foordi*, la deuxième nageoire dorsale et la nageoire anale semblent former un seul module: elles apparaissent, se développent et grandissent ensemble. Cette modularité des nageoires médianes est similaire à celle retrouvée dans le développement de tous les actinoptérygiens vivants.